R

WT-81

Copy No. 137 A

OPERATION GREENHOUSE

SCIENTIFIC DIRECTOR'S REPORT

ANNEX 1.2 DELAYED GAMMA-RAY MEASUREMENTS

PART III FILM DOSIMETER MEASUREMENTS

NUCLEAR EXPLOSIONS 1951

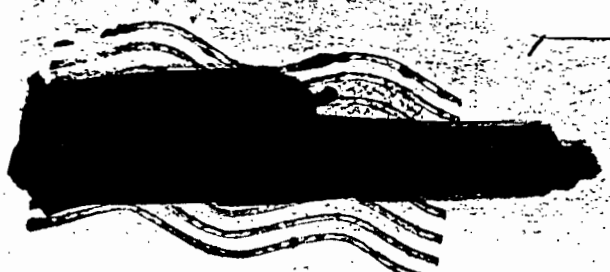

[redacted]

UNCLASSIFIED

This document consists of 72 plus 4 pages
(counting preliminary pages)
No. 137 of 150 copies, Series A

Scientific Director's Report of Atomic Weapon Tests at Eniwetok, 1951

Annex 1.2

Delayed Gamma-ray Measurements

Part III — Film Dosimeter Measurements

[redacted]

UNCLASSIFIED

This document contains restricted data as defined in the Atomic Energy Act of 1946. Its transmittal or the disclosure of its contents in any manner to an unauthorized person is prohibited.

UNCLASSIFIED

[redacted]

[redacted]

Distribution

	Copy
DEPARTMENT OF DEFENSE	
Armed Forces Special Weapons Project (Sandia)	1–3
Armed Forces Special Weapons Project (Washington)	4–15
ARMY	
Army Field Forces	16
Assistant Chief of Staff, G-3	17
Assistant Chief of Staff, G-4	18–19
Chief Chemical Officer	20–23
Chief Signal Officer	24–27
Chief of Engineers	28–32
Chief of Ordnance	33–37
Operations Research Office (Johns Hopkins University)	38–39
Quartermaster General	40–44
Surgeon General	45–46
NAVY	
Bureau of Aeronautics	47
Bureau of Medicine and Surgery	48
Bureau of Ships	49–50
Chief of Naval Operations	51
Chief of Naval Research	52
Naval Medical Research Institute	53
Naval Radiological Defense Laboratory	54–55
AIR FORCE	
Air Force Cambridge Research Center	56
Air Research and Development Command	57–60
Air Targets Division, Directorate of Intelligence (Phys. Vul. Branch)	61–62
Assistant for Atomic Energy	63
Assistant for Development Planning	64
Assistant for Materiel Program Control	65
Deputy Chief of Staff for Development (AFDRD)	66
Director of Operations (Operations Analysis Division)	67
Director of Plans (AFOPD-P1)	68
Director of Requirements	69–70
Director of Research and Development	71–72
Eglin Air Force Base, Air Proving Ground	73
Ent Air Force Base, Air Defense Command	74–75
Kirtland Air Force Base, Special Weapons Center	76–78
Langley Air Force Base, Tactical Air Command	79–80
Maxwell Air Force Base, Air University	81–82
Offutt Air Force Base, Strategic Air Command	83–85
1009th Special Weapons Squadron	86
Rand Corporation	87–88
Scott Air Force Base, Air Training Command	89–90
Wright Air Development Center	91–93
Wright Air Materiel Command	94–95
ATOMIC ENERGY COMMISSION	
Atomic Energy Commission, Washington	96–98
Los Alamos Scientific Laboratory, Report Library	99–103
Sandia Corporation	104–105
Technical Information Service, Oak Ridge (surplus)	106–149
Weapon Test Reports Group, TIS	150

[redacted]

[redacted]

DELAYED GAMMA-RAY MEASUREMENTS

Part III — Film Dosimeter Measurements

by

MARGARETE EHRLICH

WILLIAM MILLER

LAURISTON S. TAYLOR

HAROLD O. WYCKOFF

Approved by: FREDERICK REINES
Director, Program 1

Approved by: ALVIN C. GRAVES
Scientific Director

Radiation Physics Laboratory
National Bureau of Standards
Washington, D. C.

May 1952

[redacted]

Acknowledgments

The authors would like to express their appreciation to [redacted] for many valuable suggestions, to [redacted] and [redacted] for their supervision of the film processing laboratory, and to [redacted] for his work in the field.

CONTENTS

	Page
ACKNOWLEDGMENTS	v
CHAPTER 1 INTRODUCTION	1
1.1 Purpose	1
1.2 Scope	1
CHAPTER 2 SELECTION OF EMULSIONS	3
2.1 Criteria for the Selection	3
2.1.1 Emulsion Range and Accuracy	3
2.1.2 Emulsion Uniformity	3
2.2 The Final Film Selection	3
CHAPTER 3 DESIGN OF PHOTOGRAPHIC DOSIMETER	6
3.1 Requirements	6
3.2 Electronic Equilibrium Layer	6
3.3 Reduction of Energy Dependence by Means of Metallic Absorbers	8
3.3.1 History and Aims	8
3.3.2 The Modification of X-ray Spectra by Absorbers	10
3.3.3 Effect of Additional Absorbers Wrapped around Dosimeter	13
3.3.4 The Selection of Contact Absorbers to Reduce Energy Dependence	13
CHAPTER 4 CALIBRATION PROCEDURE	28
4.1 The Calibrating Radiation	28
4.1.1 Calibration Points	28
4.1.2 Dosage Rate	28
4.1.3 Radiation Filters	28
4.2 Processing	31
4.2.1 Developing	31
4.2.2 Fixing	35
4.2.3 Washing and Drying	35
4.3 Standardized Film Densitometry	35
CHAPTER 5 CALIBRATION RESULTS	37
CHAPTER 6 RESULTS OF FIELD MEASUREMENTS	43
6.1 Introduction	43
6.1.1 Accuracy of Results	43

CONTENTS (Continued)

Page

6.2 Physical Setup 45
6.3 Total Dose versus Distance — Results 45
6.4 Film Trap Measurements — Results 45
6.5 Dose Measurements in Building 311 45

ILLUSTRATIONS

CHAPTER 2 SELECTION OF EMULSIONS

2.1 Results of Calibration of 16 Photographic Emulsions with X Radiation Generated at 1.4-mev Exciting Potential 4

CHAPTER 3 DESIGN OF PHOTOGRAPHIC DOSIMETER

3.1 Electronic Equilibrium in Bakelite 7
3.2 Reduction of X-ray Dosage by Means of Metallic Absorbers 9
3.3 Path of X Radiation, Indicating Sequence of Absorbers 11
3.4 Changes of Spectrum with Filtration 14
3.5 Modification of the 250-kv Radiation Spectrum by Lead Absorbers 17
3.6 Modification of the 250-kv Radiation Spectrum by Tin Absorbers 18
3.7 Photographic Response Coefficients of the Selected Film Emulsions 20
3.8 Determination of Absorber Thicknesses Required for Reduction of Energy Dependence of Film Emulsions 23
3.9 Matching of Dosage Reductions and Du Pont Response Coefficients 24
3.10 Matching of Dosage Reductions and Eastman Response Coefficients 25
3.11 Performance Expected of the Chosen Absorber Combinations 26

CHAPTER 4 CALIBRATION PROCEDURE

4.1 Modification of 250-kv Radiation Spectrum by Means of Filters 29
4.2 Half-value Layer of X Radiation as Function of Beam Filtration Determined by Tin Absorption Measurements 30
4.3 Theoretical Spectral Distributions of the Calibrating Radiations 32
4.4 Influence of Choice of Developer on Final Film Density 34

[redacted]ON

ILLUSTRATIONS (Continued)

Page

CHAPTER 5 CALIBRATION RESULTS

5.1 Calibration of Absorber Film Badge; Exposure Range from 1 to 500 Roentgens 38
5.2 Calibration of Absorber Film Badge; Exposure Range from 20 to 10,000 Roentgens 39
5.3 Calibration of Absorber Film Badge; Exposure Range from 5000 to 100,000 Roentgens. 40
5.4 Calibration of Bare Film Packets; Exposure Range from 1 to 500 Roentgens 41
5.5 Calibration of Bare Film Packets; Exposure Range from 25 to 2500 Roentgens. 42

CHAPTER 6 RESULTS OF FIELD MEASUREMENTS

6.1 Film Badge in Various Stages of Assembly 46
6.2 Typical Setup of Total-dose, Sail, and Drop Film 47
6.3 Total Dose versus Distance for the Four Greenhouse Shots 48
6.4 Total Dose Times Distance Squared versus Distance for the Four Greenhouse Shots 49
6.5 Percentage of Film Dose Received at Various Times — Blast Initiated Film Drops 50
6.6 Percentage of Film Dose Received at Various Times — Flash Initiated Film Drops 51
6.7 Schematic of First Level, Building 311 52
6.8 Schematic of Second Level, Building 311 53
6.9 Schematic of Third Level, Building 311 54
6.10 Dose in Building 311, First Floor 55
6.11 Dose in Building 311, Second Floor 56
6.12 Dose in Building 311, Third Floor 57
6.13 Dose in Building 311, First Floor; Dosimeters Placed at Front and Rear of Columns 58
6.14 Dose in Building 311, Second Floor; Dosimeters Placed at Front and Rear of Columns 59
6.15 Dose in Building 311, Third Floor; Dosimeters Placed at Front and Rear of Columns 60

TABLES

CHAPTER 3 DESIGN OF PHOTOGRAPHIC DOSIMETER

3,1 Sample Computation of X-ray Dosage behind Filters. 12
3.2 Computation of X-ray Dosages behind Increasing Thicknesses of Lead 15
3.3 Computation of X-ray Dosages behind Increasing Thicknesses of Tin 16
3.4 Dosage Reduction Ratios for Lead and Tin 19

[redacted]

TABLES (Continued)

Page

3.5 Photographic Response Coefficients of the Four Selected Emulsions 21
3.6 Thicknesses of Absorbers Required to Make Response Coefficient of Packet Equal to Unity 22
3.7 Per Cent Inaccuracy in Dosage Interpretation in the Range from 35 to 600 Kev 27

CHAPTER 4 CALIBRATION PROCEDURE

4.1 Characteristics of the Selected Filtrations 33

[redacted]

Chapter 1

Introduction

1.1 PURPOSE

During the planning of Operation Greenhouse, the problem arose of providing a large number of experimenters with a cheap, moderately accurate dosimeter. Photographic emulsions had been used at Sandstone for similar purposes. However, because of the necessarily hurried preparation for the Sandstone tests, several refinements in the construction of the dosimeter, in its calibration, and in the evaluation of the dosimetric results had to be neglected. Even with several simplifications, many of the calibrations had to be obtained after the tests were completed.

Because the number of dosimeters requested for Greenhouse was much greater than that for Sandstone and because some applications required a small-sized dosimeter, it was decided to use the small, relatively inexpensive photographic film dosimeter again.

1.2 SCOPE

The photographic films for Operation Greenhouse were used essentially in two ways:

a. For studies of radiation intensity distributions in lucite and pressed-wood phantoms simulating bodies of men and small animals.

b. For dosimetry at locations where the knowledge of absolute dosages was required. This was the case for the determination of shielding properties of structural materials and for an evaluation of the accuracies of other instruments.

The photographic method lends itself well to absolute dosage determinations at high radiation fluxes since the response of photographic materials to X and gamma radiation has been found to be independent of the radiation flux for intensity ratios[1,2] of at least 1 : 10,000.

The National Bureau of Standards was made responsible for providing calibrated emulsions to cover the dosage range from 1 to 10,000 roentgens for all phantom and absolute dosage measurements for Operation Greenhouse. Personnel of the Bureau were also to act as consultants for all other photographic dosimetry at Greenhouse and to have the responsibility for processing all Greenhouse-exposed films. Chapter 2 of this report discusses the selection of the four photographic emulsions supplied by the National Bureau of Standards. A detailed account of the processing sequence is given in Sec. 4.2.

The densitometric results obtained in phantom work were interpreted by the Navy group. The National Bureau of Standards supplied only a calibration curve to be used by the Navy as a processing check for this application. The densitometric results obtained in the absolute dosage measurements were interpreted by the National Bureau of Standards with the aid of a photographic dosimeter specially designed and calibrated for this purpose. A large portion of this report (Chap. 3) deals therefore with the design of a photographic meter suited for this application. The meter provides electronic equilibrium over the emulsion surfaces and allows a dosage interpretation with an accuracy of ±21 per cent in the range from 122-kev effective radiation energy to the effective energy of a 10-mev betatron. This accuracy is not out of line with requirements since the greatest accuracy of the biological experiments which were checked photographically was ±15 per

[redacted]

cent. Electronic equilibrium was achieved by means of a 0.33-in. layer of bakelite, which corresponds in thickness to the average range of the electrons expected to be produced in an atomic explosion. The dosimeter's energy dependence in the low-energy region of high film sensitivity was decreased by means of metallic absorbers consisting of 0.3 mm lead and 1.07 mm of tin which reduced the intensity of the part of the radiation to which the film is most sensitive.

A detailed account of the calibration of this dosimeter and of its accuracy limits is presented in Chaps. 4 and 5.

REFERENCES

1. Russell Morgan, Reciprocity Law Failure in X-ray Films, Radiology, 42: 471-479 (1944).
2. National Bureau of Standards, unpublished data.

[redacted]

Chapter 2

Selection of Emulsions

2.1 CRITERIA FOR THE SELECTION

Photographic dosimetry is based on a unique correlation of radiation exposures and photographic densities. Since a large number of individual dosimeters were to be used, it was desirable to control the fluctuations that might occur between individual pieces of photographic film as well as to ensure that their range would be adequate to cover the expected radiation intensities. The selection of emulsions for Operation Greenhouse was therefore guided by the criteria given in Secs. 2.1.1 and 2.1.2.

2.1.1 Emulsion Range and Accuracy

The range of an emulsion useful for photographic dosimetry depends upon the saturation density of the emulsion and upon the accuracy with which emulsion blackening may be interpreted in terms of dosage in roentgens. This accuracy, in turn, is determined by the emulsion contrast (its ability to record differences in exposure in terms of differences in photographic blackening). With a given developing procedure, the saturation density and the contrast vary with the type of emulsion. Since the newest type densitometer allows the evaluation of photographic densities up to 6, emulsions with saturation densities close to or above 6 were utilized. Among these, the ones providing the best contrast and therefore the greatest accuracy in the range from 1 to 10,000 roentgens were chosen.* For some particular phases of the work this range was extended up to 100,000 roentgens.†

*Eastman 5302 and 548-0, double coat, and Du Pont 510 and 605.

†Eastman 548-0, single coat.

2.1.2 Emulsion Uniformity

Large manufacturers of photographic materials are able to control the uniformity of each individual film within a given emulsion batch to an accuracy exceeding that obtained in other phases of photographic dosimetry. However, the variations between different emulsion batches may cause significant changes in the X- and gamma-ray sensitivity of these emulsions, thus making it necessary to obtain all films of a given type from the same emulsion batch.

2.2 THE FINAL FILM SELECTION

Sixteen different film emulsions were calibrated over their entire useful exposure range with X radiation of 1.4-mev exciting potential having a half-value layer of 10.4 mm of tin and an effective energy of approximately 600 kev. In this energy region, the response of the photographic emulsions is essentially independent of the quantum energy of the incident radiation. The X-ray intensities were measured with a Victoreen roentgen meter with walls of electronic equilibrium thickness. The exposed films were developed in Eastman X-ray developer which was also chosen for the Greenhouse work (see Sec. 4.2.1). Figure 2.1 shows the calibration results graphically.

The Eastman spectroscopic film 548-0, double coat, was the only film which covered the dosage range from 500 to 10,000 roentgens with adequate accuracy. The Defender Ad-Lux film was not considered because of its low saturation density and its low contrast in the exposure region between 1000 and 10,000 roentgens. Three emulsions covered the range

[redacted]

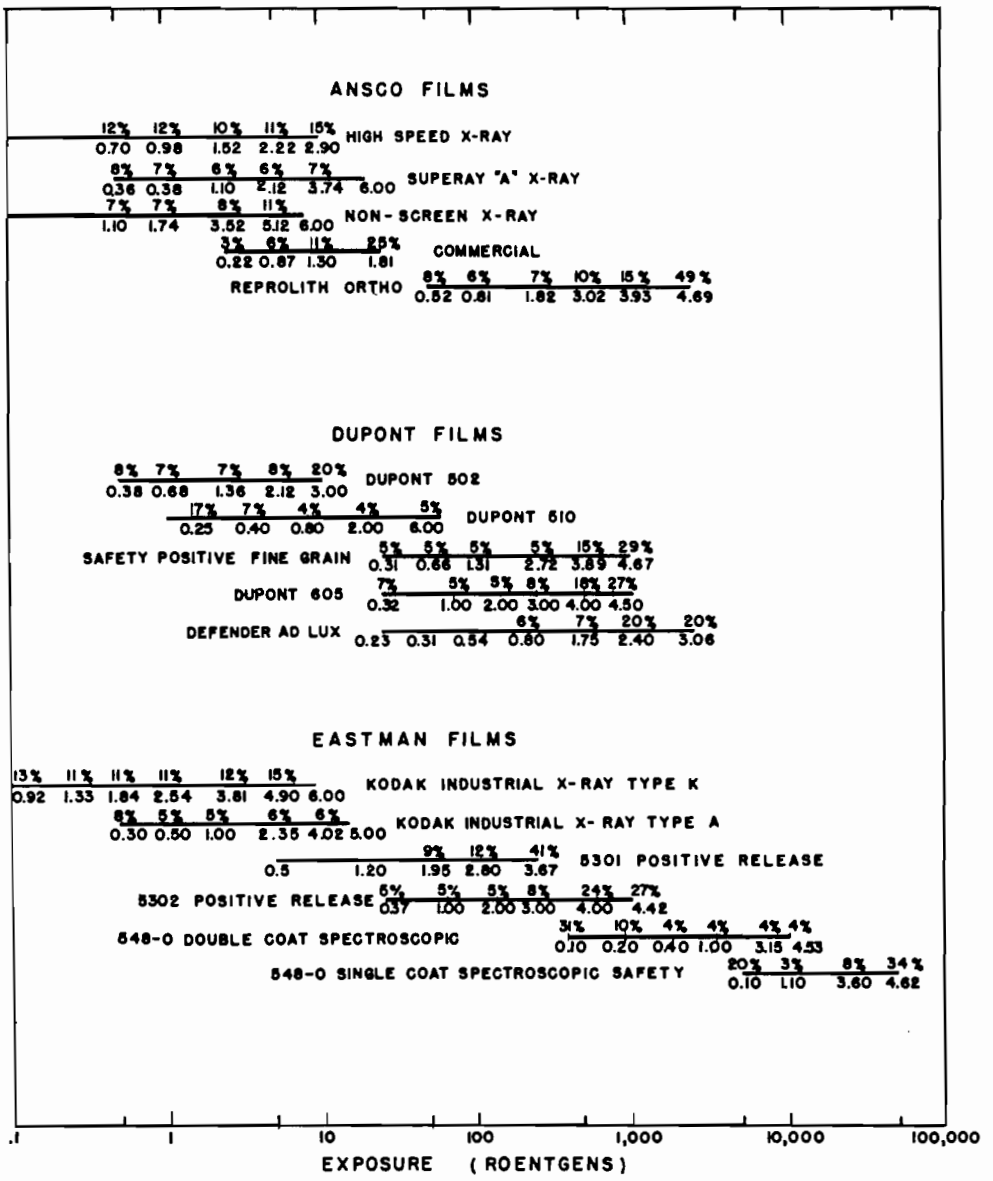

Fig. 2.1 Results of Calibration of 16 Photographic Emulsions with X Radiation Generated at 1.4-mev Exciting Potential. The logarithms of the X-ray exposures in roentgens are plotted horizontally; the numbers below the horizontal lines represent the photographic densities at the particular points; the numbers above the lines represent the accuracies of the emulsions in per cent at the particular radiation dosages. The accuracies were obtained by calculating the percentage of the total exposure in roentgens corresponding to a density variation of 5 per cent or 0.02 density unit, whichever was larger. This variation was accepted as the inherent inaccuracy of the calibration procedure.

[redacted]

from 30 to 500 roentgens: Ansco Reprolith orthochromatic, Du Pont safety positive, and Du Pont 605. The Ansco film was excluded because experiments had shown that it fogs in the Wratten safelight 6B which is safe for use with all other films. The Du Pont 605 film was selected. For the coverage of the range from 1 to 50 roentgens, Du Pont 510 was chosen, even though it overlaps slightly with the Du Pont 605 film. This provides a useful check on the performance of these two films. Also, as a performance check, Eastman 5302 positive film was added to the selection.

The four selected films, in standard dental packets, constitute the essential part of the film dosimeter. However, for the determination of radiation dosages above 10,000 roentgens, two of these films were replaced by the Eastman 548-0 single-coat film, also in a dental packet.

[redacted]

[redacted]

Chapter 3

Design of Photographic Dosimeter

3.1 REQUIREMENTS

The four photographic films whose selection was described in Chap. 2 record primary and secondary X and gamma radiation, slow and fast neutrons, secondary electrons stemming from surrounding irradiated structures, and all other secondary ionizing fragments which may reach the emulsion surface. However, it was expected that significant film blackening at Greenhouse would stem only from irradiation with gamma radiation and electrons. An order-of-magnitude calculation based on the experimental data of Kalmon[1] obtained on unshielded Du Pont 552 films with fast neutrons from a polonium-beryllium source showed that the blackening expected from neutrons at a given station was negligible compared to the blackening caused by the gamma radiation at the same location. As discussed in Secs. 3.2 and 3.3, a large number of the film packets to be used at Greenhouse had to be enclosed in bakelite holders covered with layers of lead and tin. An additional increase of film blackening was therefore expected due to elastic and inelastic scattering of neutrons in the lead and tin and especially from neutron-proton scattering in the bakelite. Recent experiments by T. E. Shea, Jr., indicated, however, that these additional effects were negligible.[2] The blackening caused by secondary electrons was considered in the calibration of the film emulsions, and a method was devised to make the electron flux reproducible. The details of this work are discussed in Sec. 3.2.

3.2 ELECTRONIC EQUILIBRIUM LAYER

The number of electrons actually passing through the film emulsions depends upon the atomic number and density of the material in which they are produced. In order to standardize the electron flux through the emulsions, it was therefore necessary to surround the entire film packet with a layer of substance of a low atomic number and of a thickness approximately equal to the maximum range of the secondary electrons expected from the gamma rays of an atomic explosion. Bakelite was chosen because of its good heat-resistive qualities. The bakelite thickness was determined experimentally under the assumption that the spectrum from a 10-mev betatron is similar to that of the bomb (see Greenhouse Report, Annex 1.2, Part I).

Electrons formed outside this layer are absorbed, whereas electrons formed within the layer itself reach the film emulsion. In this way, the point-to-point variation of the total energy absorbed in the layer is made to parallel roughly the absorption of X and gamma rays. This situation is usually referred to as electronic equilibrium. The response of emulsions exposed under conditions of electronic equilibrium is independent of electrons scattered from nearby structures.

The way in which the film density caused by a given exposure varies with the thickness of the shielding layer is illustrated in Fig. 3.1, which shows the results of an experiment designed to determine the absorber thickness needed for electronic equilibrium of Co^{60} gamma radiation. Bakelite was used as an absorber. The density of Ansco Commercial film exposed to a fixed radiation dose is plotted against the thickness of the bakelite layer introduced over the emulsion surface. In the first portion of the curve, the film density is seen to increase mark-

[redacted]

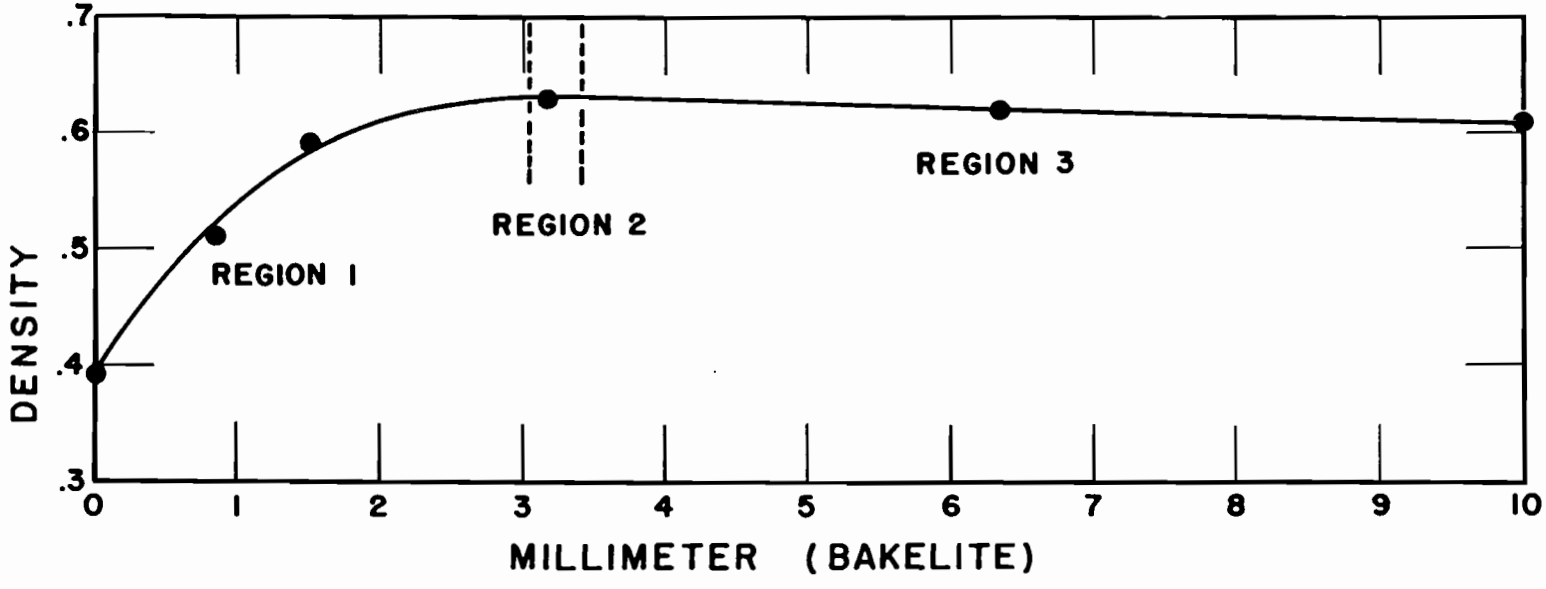

Fig. 3.1 Electronic Equilibrium in Bakelite

edly with increasing bakelite thickness. This shows that the bakelite thickness is not sufficient for electronic equilibrium and that the number of electrons reaching the emulsion increases with the bakelite thickness. (In the experiment, electron emission and scatter from the installation were eliminated. Otherwise, the film density could very easily be found to decrease with absorber thickness below electronic equilibrium. This would be the case if the number of extraneous electrons shielded from the emulsion by the added bakelite were larger than the number of electrons emitted from it.)

In the second region, the curve flattens and reaches a somewhat indistinct maximum corresponding to the region of electronic equilibrium.

The third region is characterized by a gradual decrease of density with absorber thickness, corresponding to the attenuation of the primary radiation within the bakelite.

If the bakelite thickness which corresponds to region 2 in Fig. 3.1 is used over the film packets exposed to low-energy X radiation, a slight attenuation of the primary beam occurs. However, this factor was inappreciable for the Greenhouse operations.

3.3 REDUCTION OF ENERGY DEPENDENCE BY MEANS OF METALLIC ABSORBERS

3.3.1 History and Aims

The response of all presently available photographic emulsions varies with energy in the neighborhood of the silver and bromine absorption edges. This complicates the use of photographic emulsions for X-ray and gamma-ray dosimetry over wide quantum energy ranges.[3,4] Thus, whenever the radiation incident on a film dosimeter has components in the quantum energy range of these absorption edges, it is impossible to interpret film densities in terms of radiation dosage as measured in roentgens unless the radiation spectrum is known. Various attempts have been made to bypass this difficulty and to design film meters which would be useful for dosage determinations of radiation of unknown quality.

Tochilin et al.,[5] Baker and Silverman,[6] and other authors have suggested film badges in which several different metallic absorbers are used side by side in contact with the film packet. The film density readings are interpreted with the aid of tables relating the ratios of densities under the different absorbers to the dosage in roentgens received by the film. This method seems cumbersome and inaccurate, especially because of the unavoidable effects of scattering from absorbing materials close to the film packet. The same holds for the lead cross packets used at Sandstone. Earlier, Pardue et al.[7] and Deal et al.[8] attempted to compensate for the film response peak by introducing a thin layer of cadmium over the film surface. Pardue and his co-workers determined the thickness of the cadmium shield experimentally for the particular films under consideration. Deal and his co-workers used the same cadmium thickness in their calibration of the Du Pont 552 experimental film packet.

The work carried out at the National Bureau of Standards was based on the same assumption as was that of Pardue and Deal, namely, that it was possible to make the film response independent of radiation quality by means of metallic absorbers covering the entire emulsion surface. The required absorber thicknesses were determined by a graphical method and checked experimentally.

Since the photographic effect is determined to a considerable extent by the absorption of X rays in silver bromide, the photographic response curve should resemble an absorption curve in its trend. The ratios of the dosage in the absence of an absorber (D_{wo}) to the corresponding dosage behind the absorber (D_w) for different exciting potentials and for different absorbers are plotted in Fig. 3.2. A typical photographic response curve is shown on the same graph. The ordinate represents the ratio of the dosage in roentgens necessary to produce a given photographic density in the million-volt range, where the film response is energy independent, to the dosage needed to produce the same density at a specified low exciting potential. This ratio will be referred to as the photographic response coefficient. If the curve of D_{wo}/D_w for any absorber or combination of absorbers matches the photographic response curve, it could be expected that this absorber placed in front of the film packet would yield a

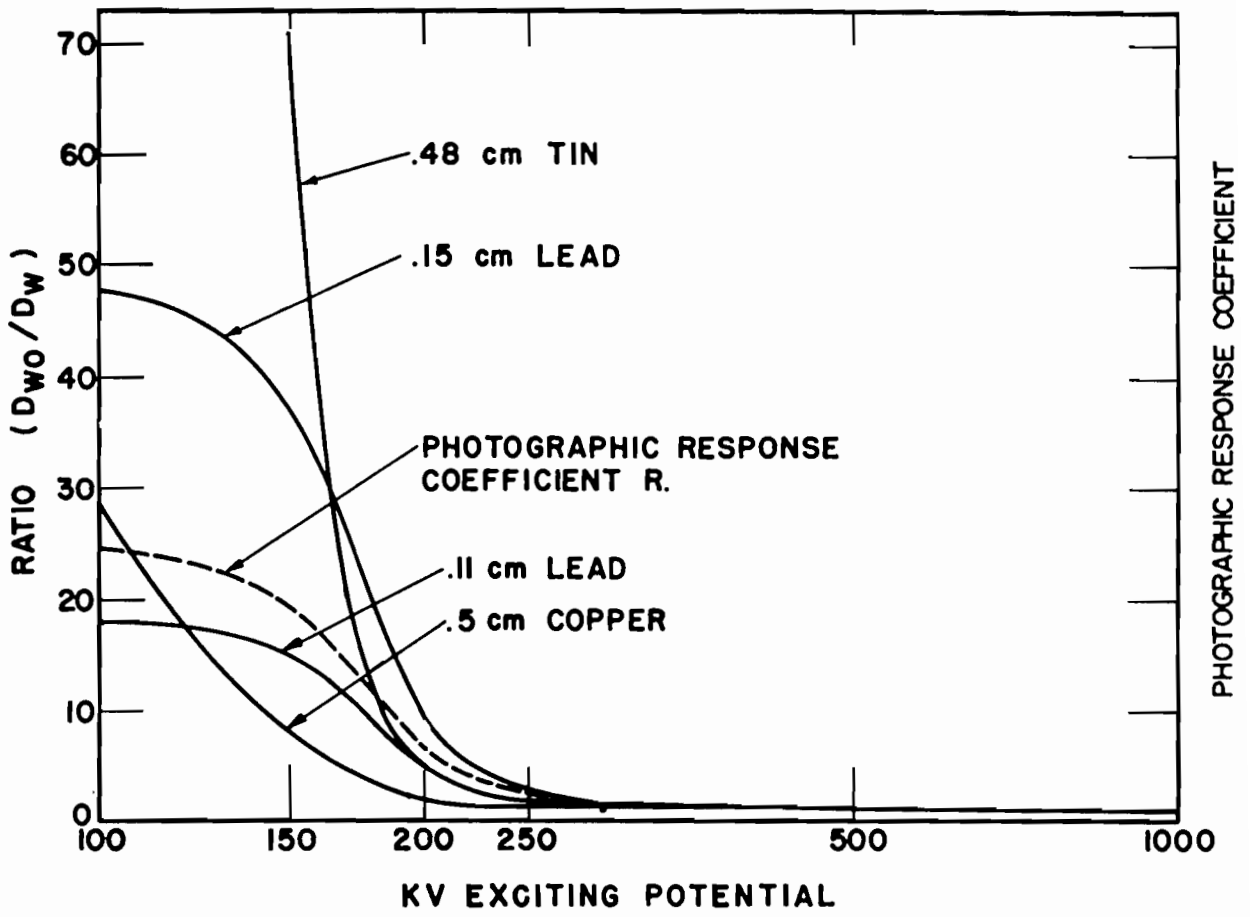

Fig. 3.2 Reduction of X-ray Dosage by Means of Metallic Absorbers

net response which is approximately energy independent.

It will be shown in the next section how the ratio D_{wo}/D_w can be estimated theoretically, thus avoiding extensive experimentation. The results obtained in this way are applied in Sec. 3.3.3 to the selection of an absorber of the desired characteristics.

3.3.2 The Modification of X-ray Spectra by Absorbers

In order to develop the technique for the evaluation of different filter combinations, the calculations leading to the dosage ratios, D_{wo}/D_w, will be outlined.

The calculations were carried out for heterochromatic X radiation from a constant potential X-ray machine. This type of source was actually used in the dosimeter calibration because monochromatic sources were not available in sufficient quantities in the particular energy regions. The width of the energy bands was made as narrow as conditions permitted. The selection of the calibrating radiation is discussed in detail in Chap. 4.

The detailed spectrum of the X radiation emerging from an X-ray tube target is generally unknown. It is, however, possible to gain valuable information regarding the spectral modification and dosage reduction caused by absorption by assuming a simple, idealized spectral distribution.

According to Kramers's theoretical formula,[9] the energy between E and E + dE emitted per electron impact is given by

$$I(E)\,dE = -C(E - E_0)\,dE \qquad (3.1)$$

which represents a straight line with the constant slope $-C$ in an intensity-versus-energy graph. This idealization is not unrealistic since the formula is in good agreement with Kulenkampff's experimental results.[10]

Figure 3.3 is a schematic representation of the path of the X radiation from its origin in the target through the different filter materials and to its absorption in the dosimeter. Another block, representing the filtration by the air intervening between the tube and the dosimeter, should actually be introduced in this diagram. However, the filtration by air is negligible in the present example.

If $I_0(E)\,dE$ is the spectral intensity distribution in the photon energy interval dE as represented by Kramers's formula and $I_1(E)\,dE$ is the intensity distribution in the same interval after its attenuation and distortion by the inherent tube filtration, then

$$I_1(E)\,dE = I_0(E)\,\exp\left[-\mu_1(E)x_1\right]dE \qquad (3.2)$$

where $\mu_1(E)$ is the linear absorption coefficient and x_1 is the thickness in centimeters of the equivalent X-ray tube filter. If $I_2(E)\,dE$ represents the spectral intensity distribution in the given energy interval dE after the passage of the X-ray beam through the added filtration of thickness x_2 and of linear absorption coefficient $\mu_2(E)$, then

$$I_2(E)\,dE = I_1\,\exp\left[-\mu_2(E)x_2\right]dE \qquad (3.3)$$

If an X-ray beam characterized by the spectrum $I_2(E)$ falls on a free-air ionization chamber, each portion dE of the spectrum contributes to the dosage D, as measured in roentgens, an amount dD which is proportional to the fraction of the beam intensity within dE which is absorbed by the air of the ionization chamber. Below the pair-production threshold, this fraction is given by the intensity $I_2(E)\,dE$ multiplied by the corresponding air absorption coefficient $\mu(E) - \sigma_s(E)_{air}$. Thus $D \propto (\mu - \sigma_s)_{air}\, I_2(E)\,dE$. The fraction of the primary beam intensity removed from the beam by scattering is represented by $\sigma_s(E)$. In the definition of the roentgen, the contribution of scattered photons to absorption is neglected, and $\sigma_s(E)$ is therefore subtracted from the total linear absorption coefficient.

Thus the total dosage is expressed in the form:

$$D \propto \int_0^{E_0} I_2(E)\left[\mu(E) - \sigma_s(E)\right]_{air} dE \qquad (3.4)$$

Table 3.1 shows a set of sample computations made for an X-ray beam generated at 200-kv exciting potential, passing through an inherent filtration equivalent to 3 mm of aluminum and through an initial beam filter of 1.96 mm of lead. The spectral intensity distributions $I_0(E)$, $I_1(E)$, and $I_2(E)$ are expressed in the same arbitrary units. The last column gives the differential dosage contributions, dD/dE, of the spectral

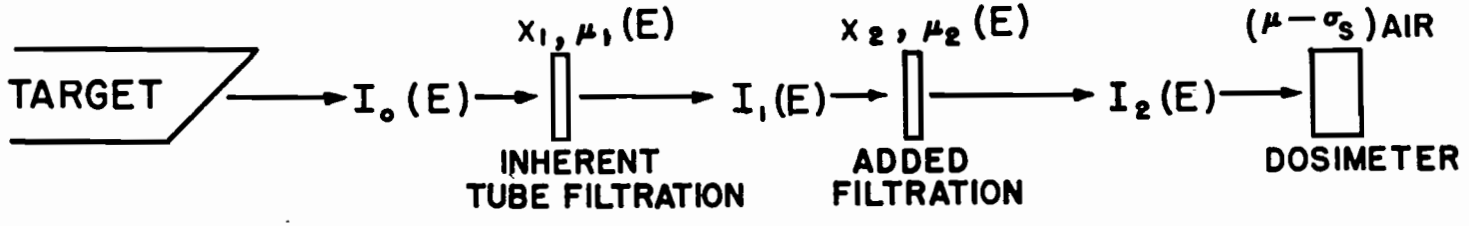

Fig. 3.3 Path of X Radiation, Indicating Sequence of Absorbers

[redacted]

TABLE 3.1 SAMPLE COMPUTATION OF X-RAY DOSAGE BEHIND FILTERS

Kev	$I_0 \times 10^{-3}$	$I_1 \times 10^{-3}$	I_2	dD/dE
0	200			
10	190	0.00000102		
20	180	1.10		
30	170	68.0		
40	160	101		
50	150	110		
60	140	110	2.25	0.0841
70	130	108	94.9	3.07
80	120	101	780	23.9
87	113		2540	77.0
89	111		0.0072	0.000217
90	110	94.5	0.0117	0.000355
100	100	87.0	0.590	0.0179
110	90	79.4	8.28	0.256
120	80	71.2	51.2	1.60
130	70	62.3	172	5.47
140	60	54.0	444	14.3
150	50	45.0	790	25.9
160	40	36.0	1160	38.4
170	30	27.0	1450	48.4
180	20	18.0	1410	47.7
190	10	9.00	1000	34.3

[redacted]

components $I_2(E)$. The differential dosages are again expressed in arbitrary units.

Figure 3.4 shows graphically the progressive changes of the spectrum at 200-kv exciting potential. The inherent filtration cuts off the softest radiation, the lead filtration suppresses the lower energies more strongly than the higher ones, except in the portion of the spectrum immediately below the K-absorption edge, and the curve dD/dE parallels roughly the curve $I_2(E)$ because $\mu(E) - \sigma_s(E)_{air}$ is fairly constant in the energy range in which $I_2(E)$ is appreciably different from zero.* The total dosage, D, is represented by the area under the curve dD/dE which was evaluated planimetrically.

3.3.3 Effect of Additional Absorbers Wrapped around Dosimeter

Any additional absorber introduced between the lead filter and the dosimeter further reduces the dosage and hardens the X-ray beam as well. Therefore, in order to reduce the spectral components of the radiation to which the film emulsions are selectively responsive, metallic absorbers were used in immediate contact with the measuring device outside the equilibrium shell. A tentative method was developed for the evaluation of their effective absorption by means of a correction $\sigma_{sf}(E)$ to the linear absorption coefficient $\mu(E)$. This correction represents the fraction of the total absorption coefficient stemming from the degraded Compton photons scattered in the forward direction. These photons are, to a large extent, not absorbed in the filters, and, as a first approximation, $\sigma_{sf}(E)$ is therefore subtracted from the total absorption coefficient. The total dosage read behind the additional absorbers is then given by

$$D \propto \int_0^{E_0} I_2(E) \left[\mu(E) - \sigma_s(E)\right]_{air} \exp\left[-(\mu - \sigma_{sf})_{abs} \, x_{abs}\right] \quad (3.5)$$

*At energies below 50 kev, the absorption coefficient $\mu(E) - \sigma_s(E)_{air}$ rises sharply. This fact causes a marked rise of the dD/dE curve below 50 kev for X-ray spectra with strong components in this energy range and thus a distortion of the total dosage measurements.

Calculations were made for various thicknesses of lead and tin. Tables 3.2 and 3.3 show sample computations of the differential dosages, dD/dE, for different thicknesses of lead and tin absorbers at 250 kv.

The data are plotted in Figs. 3.5 and 3.6. The curve representing the differential dosages measured without any additional absorber is included for reference on both graphs. Similar calculations were carried out on both elements for 100-, 150-, and 200-kv exciting potentials. A comparison between the tin and lead curves shows clearly that below the lead K-edge the absorption by tin exceeds the absorption by lead and that above the K-edge lead is more effective.

Planimetry of the areas under all curves yields the total dosages to be measured behind the absorbers. The dosage reduction ratios, D_{wo}/D_w, are calculated from the total dosages. Table 3.4 shows D_{wo}/D_w for the two absorbers at four different exciting potentials.

3.3.4 The Selection of Contact Absorbers to Reduce Energy Dependence

In Fig. 3.7 are plotted the photographic response coefficients of the four selected emulsions versus the half-value layer of the calibrating radiation. The photographic response coefficients were calculated from the calibration data as r_2/r_1, where r_1 was the dosage to which an emulsion was exposed at a specified low voltage and r_2 was the dosage yielding the same density at a specified higher voltage as r_1 produced at the low voltage. The densities corresponding to both r_1 and r_2 were in the linear range of the characteristic curves, except in the case of the Eastman 548-0 film, where the dosages r_1 and r_2 were in the low density range in which this film was actually used. The response coefficients determined in this way are listed in Table 3.5.

In order to determine the absorbers which would make the coefficients equal to unity in the specified quantum energy range, these coefficients have to be matched against the dosage reduction ratios, D_{wo}/D_w, of Table 3.4. Instead of matching the curves visually, as indicated in Fig. 3.2, the required absorber thicknesses were taken directly from a D_{wo}/D_w versus centimeter thickness graph shown in

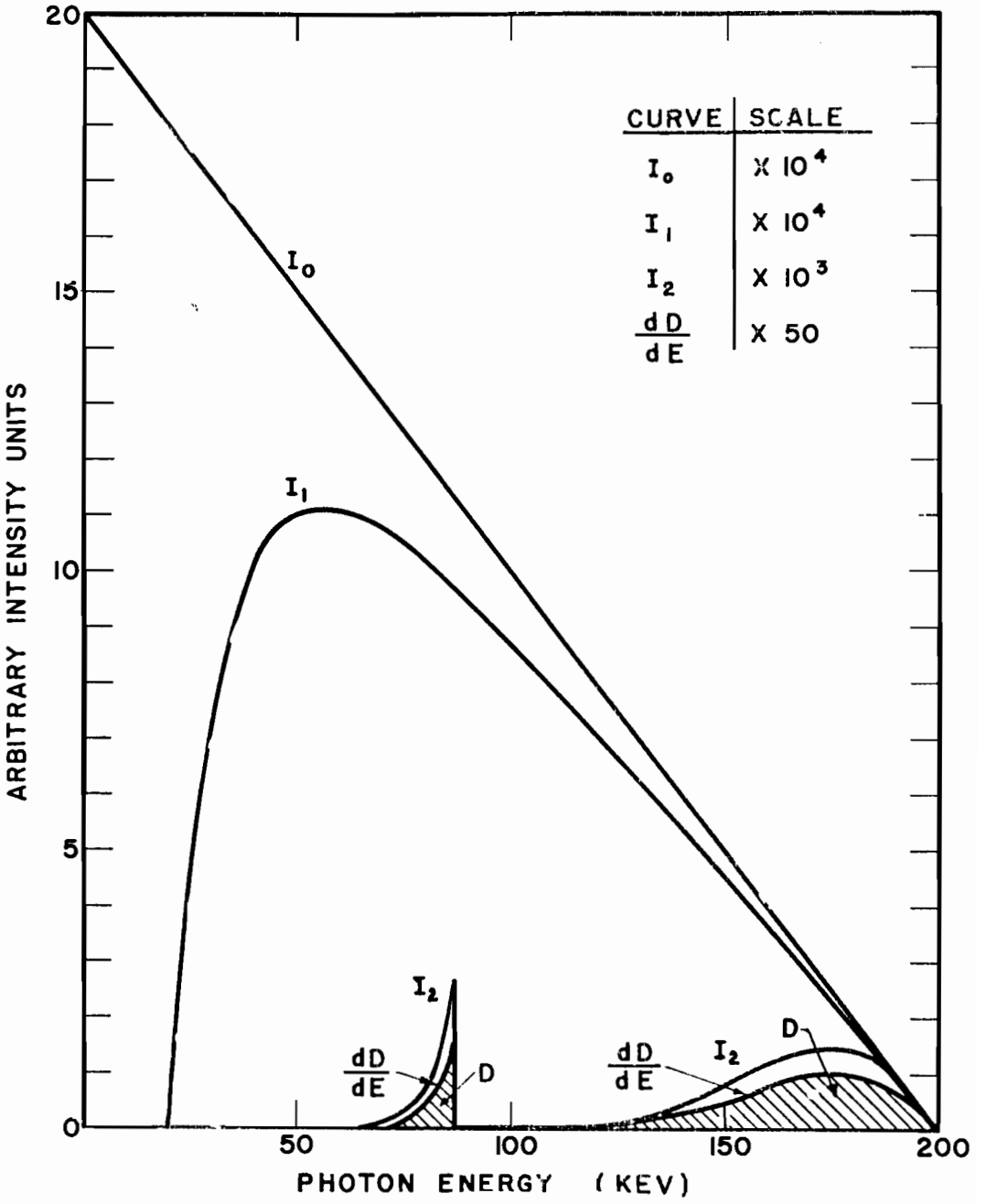

Fig. 3.4 Changes of Spectrum with Filtration

[redacted]

TABLE 3.2 COMPUTATION OF X-RAY DOSAGES BEHIND INCREASING THICKNESSES OF LEAD

	dD/dE behind Lead Absorbers			
Kev	0.03 cm Pb	0.05 cm Pb	0.11 cm Pb	0.15 cm Pb
80	0.0151	0.00936	0.00272	0.000841
87	0.0955	0.0670	0.0230	0.00112
90				
100				
110	0.000294	0.000117	0.00000737	0.00000115
120	0.00325	0.00158	0.000181	0.0000423
130	0.0175	0.00968	0.00164	0.000505
140	0.0689	0.0428	0.00930	0.00395
150	0.162	0.109	0.0326	0.0148
160	0.352	0.252	0.0912	0.0462
170	0.562	0.422	0.181	0.101
180	0.827	0.647	0.309	0.186
190	1.06	0.860	0.456	0.298
200	1.26	1.05	0.600	0.412
210	1.39	1.18	0.720	0.519
220	1.33	1.16	0.750	0.606
230	1.10	0.970	0.658	0.507
240	0.636	0.566	0.400	0.316

[redacted]

TABLE 3.3 COMPUTATION OF X-RAY DOSAGES BEHIND INCREASING THICKNESSES OF TIN

	dD/dE behind Tin Absorbers		
Kev	1.5 mm Sn	4.8 mm Sn	6.3 mm Sn
80	0.00115		
87			
90			
100			
110	0.000295	0.0000139	
120	0.00321	0.000284	0.00000354
130	0.00756	0.00252	0.00104
140	0.0680	0.0137	0.00654
150	0.163	0.0444	0.0244
160	0.354	0.117	0.0712
170	0.561	0.218	0.141
180	0.829	0.361	0.249
190	1.07	0.527	0.383
200	1.27	0.678	0.507
210	1.39	0.792	0.617
220	1.35	0.833	0.673
230	1.09	0.692	0.568
240	0.633	0.419	0.351

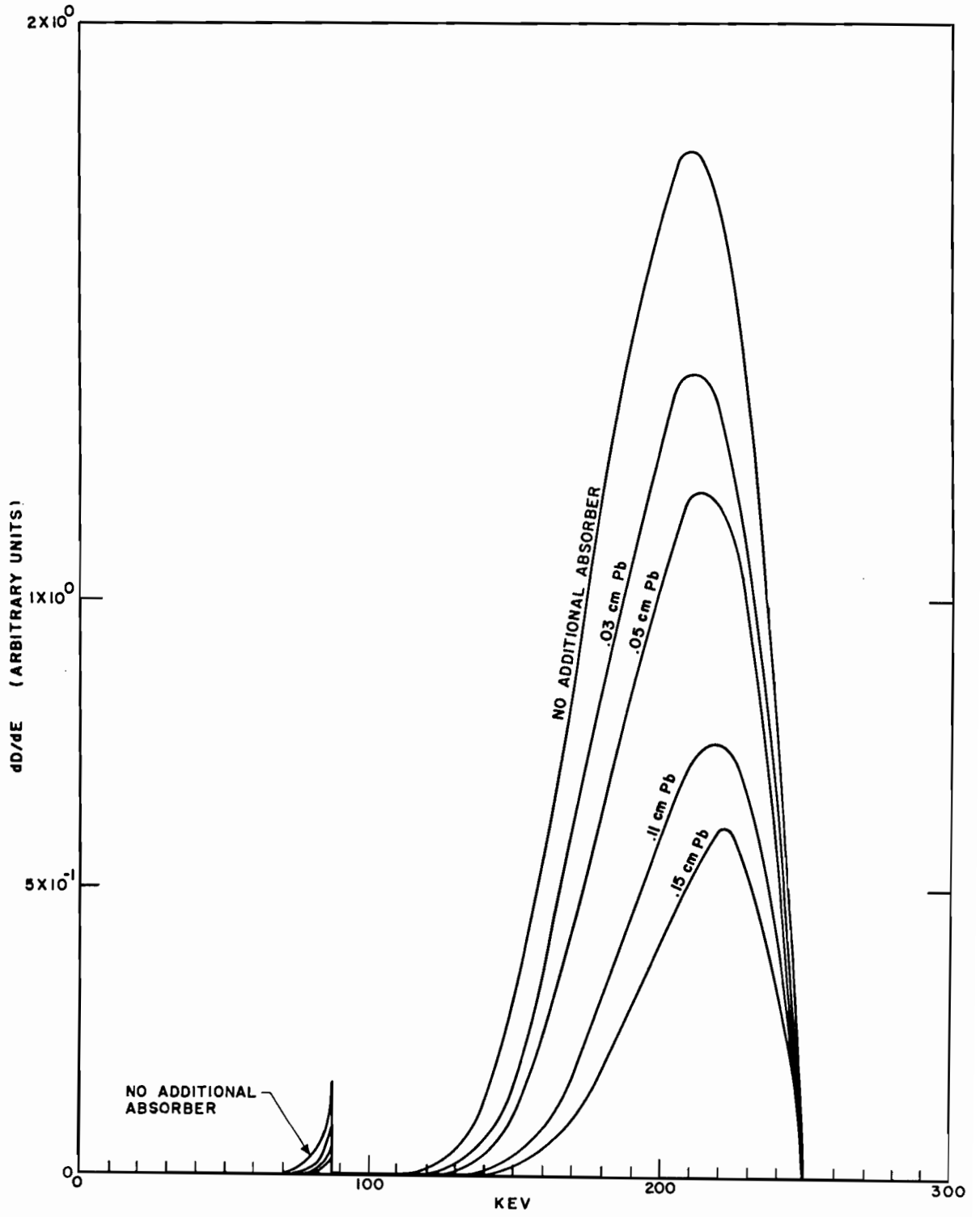

Fig. 3.5 Modification of the 250-kv Radiation Spectrum by Lead Absorbers

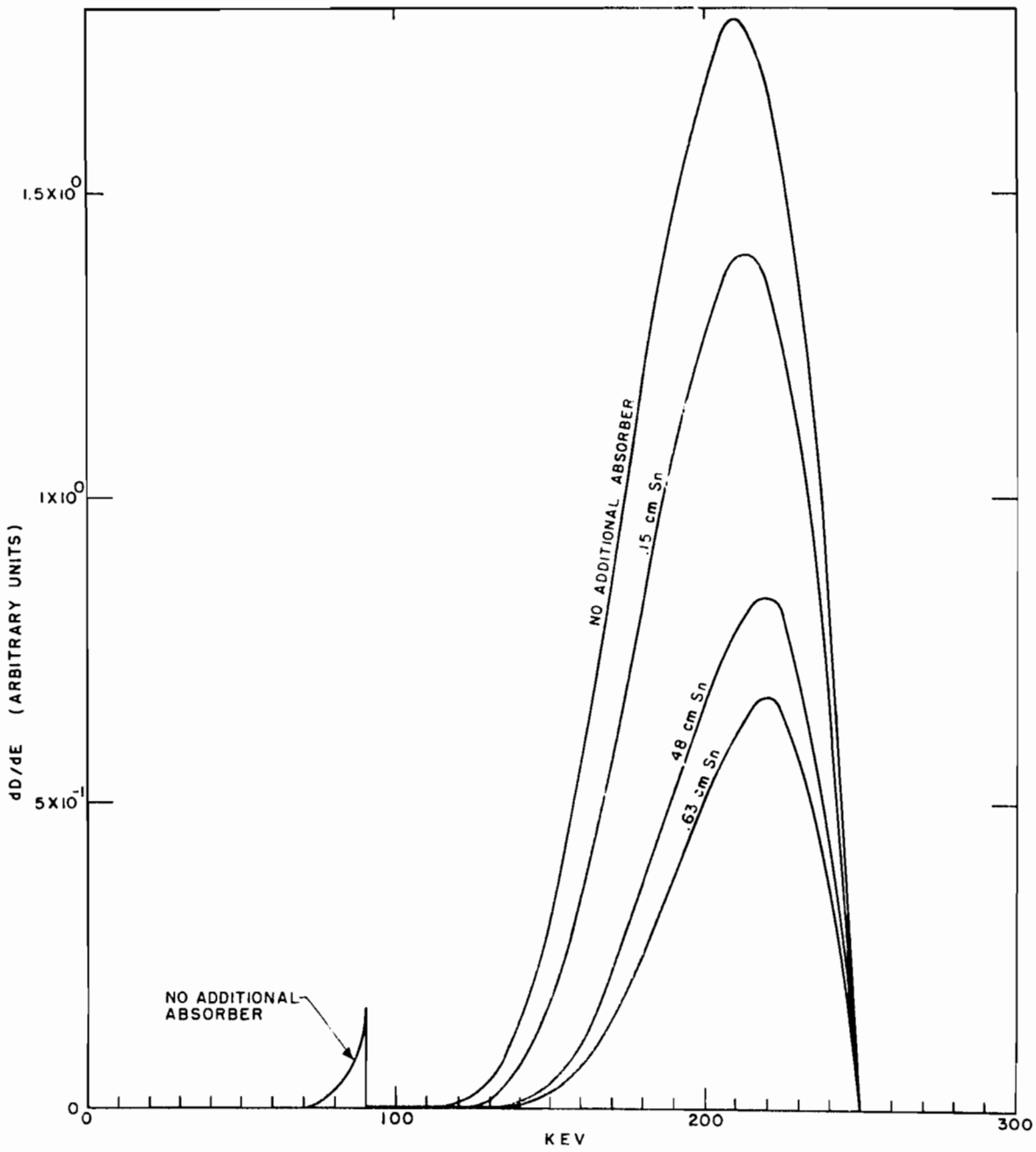

Fig. 3.6 Modification of the 250-kv Radiation Spectrum by Tin Absorbers

TABLE 3.4 DOSAGE REDUCTION RATIOS FOR LEAD AND TIN

Absorber Element	Absorber Thickness (cm)	D_{wo}/D_w At 100 kv	At 150 kv	At 200 kv	At 250 kv
None	None	1	1	1	1
Lead	0.03	3.45	2.90	1.61	1.35
	0.05	6.70	5.67	2.21	1.64
	0.11	34.3	34.6	5.43	2.81
	0.15	95.2	100	10.43	3.96
Tin	0.02	1.82			
	0.05	4.17			
	0.11	13.85			
	0.15	40.70	2.96	1.53	1.34
	0.48		24.8	4.28	2.48
	0.63		58.2	6.79	3.38

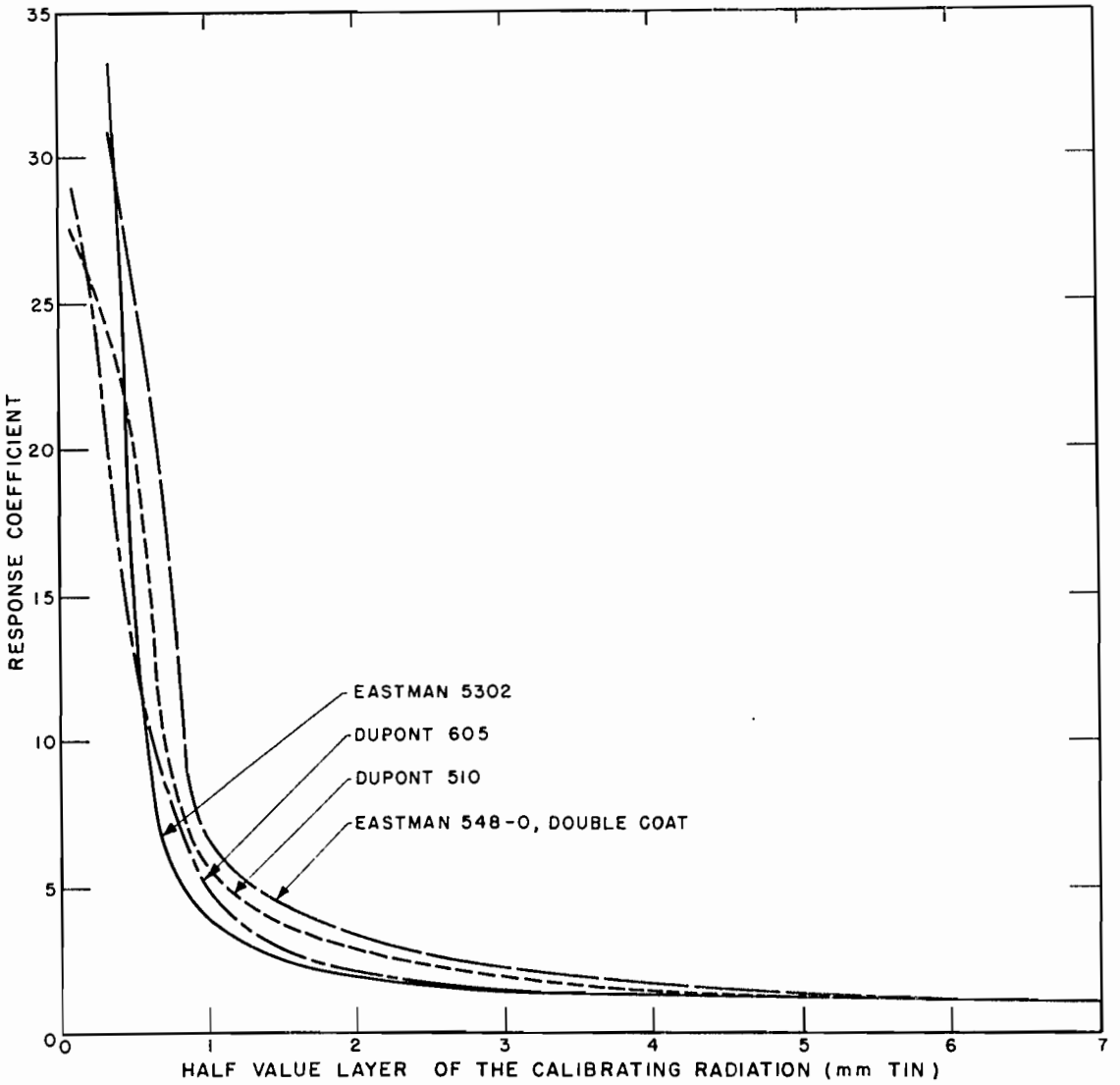

Fig. 3.7 Photographic Response Coefficients of the Selected Film Emulsions

TABLE 3.5 PHOTOGRAPHIC RESPONSE COEFFICIENTS OF THE FOUR SELECTED EMULSIONS

Radiation Quality		Response Coefficients			
Exciting Potential (kv)	Half-value Layer (mm Sn)	Du Pont 510	Du Pont 605	Eastman Positive 5302	Eastman Spectroscopic 548-0 (Double Coat)
500–1400	6.4–11.3	1	1	1	1
250	3.64	2	1.55	1.17	2
200	2.19	2.8	2.05	2.40	3.33
150	1.01	5.5	4.9	3.33	6.56
100	0.33	23.6	19.0	>33.3	30.8
50	0.08	27.5	29		

TABLE 3.6 THICKNESSES OF ABSORBERS REQUIRED TO MAKE RESPONSE COEFFICIENT OF PACKET EQUAL TO UNITY

Exciting Potential (kv)	Thicknesses of Absorber (cm)			
	Lead	Tin	Lead	Tin
	Du Pont 510		Du Pont 605	
100	0.093	0.135	0.084	0.125
150	0.049	0.222	0.046	0.210
200	0.069	0.332	0.046	0.235
250	0.071	0.350	0.049	0.266
	Eastman Cine Positive 5302		Eastman Spectroscopic 548-0 (Double Coat)	
100	0.108	0.146	0.105	0.144
150	0.33	0.169	0.054	0.245
200	0.54	0.282	0.075	0.392
250	0.22	0.100	0.071	0.350

Fig. 3.8. The thicknesses determined in this way are listed in Table 3.6; they vary considerably with the exciting potentials.

It was then attempted to find a filter for each of the emulsions which would fit all four exciting potentials. For better visualization, the pertinent reduction ratio curves are plotted along with the film response curves in Figs. 3.9 and 3.10. The figures show that, while the lead reduction curves parallel the response curves in the range from 200- to 250-kv exciting potential, the lead reduction is insufficient at lower voltages. On the other hand, a tin absorber alone is seen to be satisfactory only for the Eastman positive film 5302. For the three other emulsions, the tin absorber which looks satisfactory above 200 kv is too thick at lower exciting potentials. It was therefore expected that for these three films a combination of tin and lead would be more suitable.

The effect of various combinations was calculated. Figure 3.11 shows the performance expected of the best combination for each film type. These combinations seemed to suppress the response at 100 kv more than desired but seemed satisfactory otherwise. However, since all four emulsions were to be combined in one dosimeter, a further compromise had to be made. An absorber combination of 1.07 mm of tin and 0.3 mm of lead was finally selected. The absorbers were placed over the bakelite film container, tin in contact with the bakelite and the lead covering the tin, in order to stop the lead fluorescent radiation in the tin absorber. A lead strip, approximately 0.78 mm thick, was wrapped around the periphery of the badge to protect the films from tangential radiation and at the same time cover the badge seam.

Table 3.7 shows the results of a calibration of this badge at radiation energies between 35 and 600 kev. As was expected, the response of all the films is too much suppressed below 122 kev, and the response of Eastman 5302 is too much suppressed throughout the entire interval. The other three films, however, allow a dosage interpretation accurate within 25 per cent over the energy range from 122 to 600 kev. The fact that the Eastman 5302 film underreads about 25 per cent between 172 and 210 kev and the Du Pont 605 film which covers the same dosage interval reads right within 7 per cent made it possible to draw conclusions regarding the radiation components in this spectral range (see Greenhouse Report, Annex 6.5).

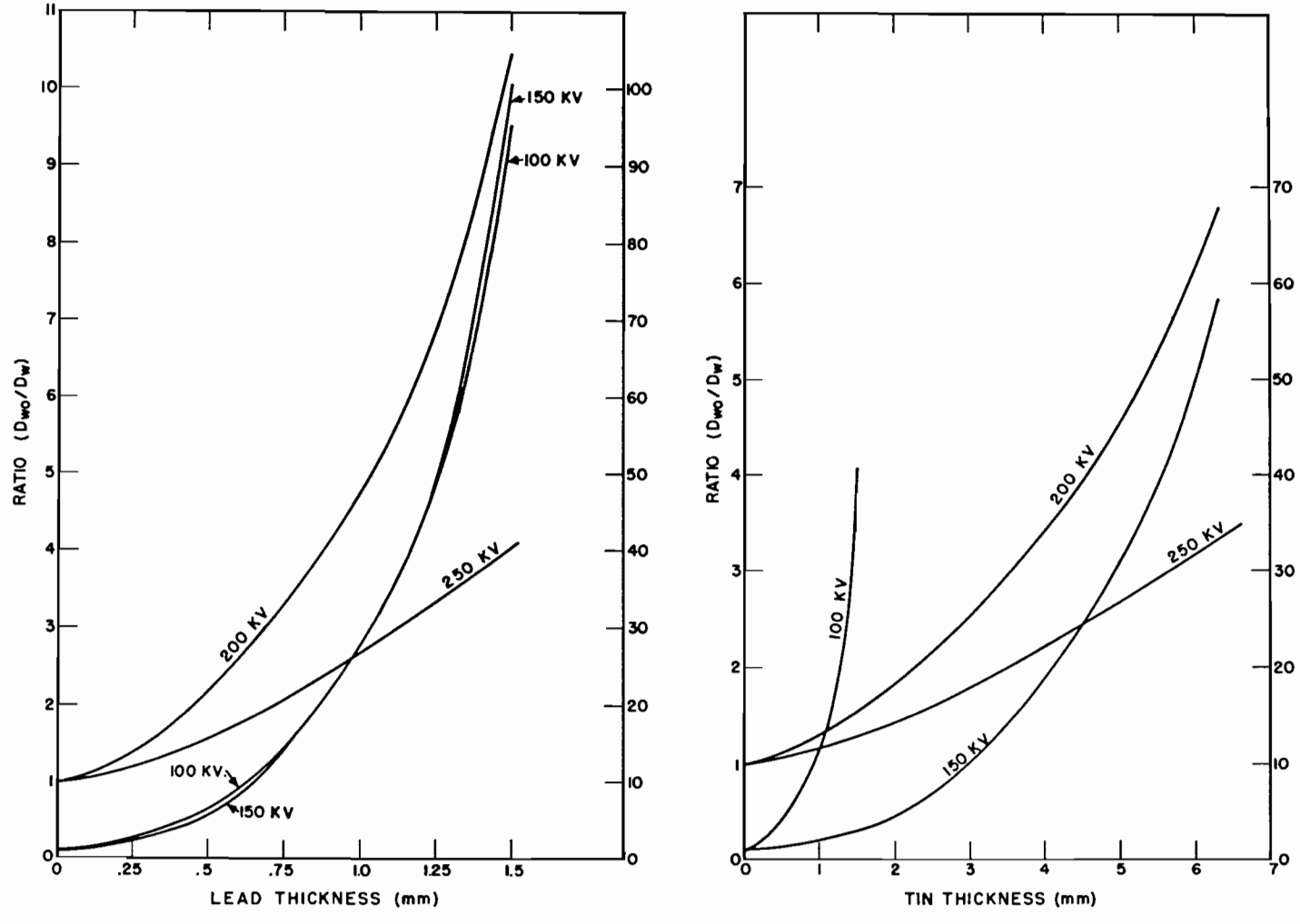

Fig. 3.8 Determination of Absorber Thicknesses Required for Reduction of Energy Dependence of Film Emulsions. The ordinates on the left apply to the 200- and 250-kv curves, and the ones on the right apply to the 100- and 150-kv curves.

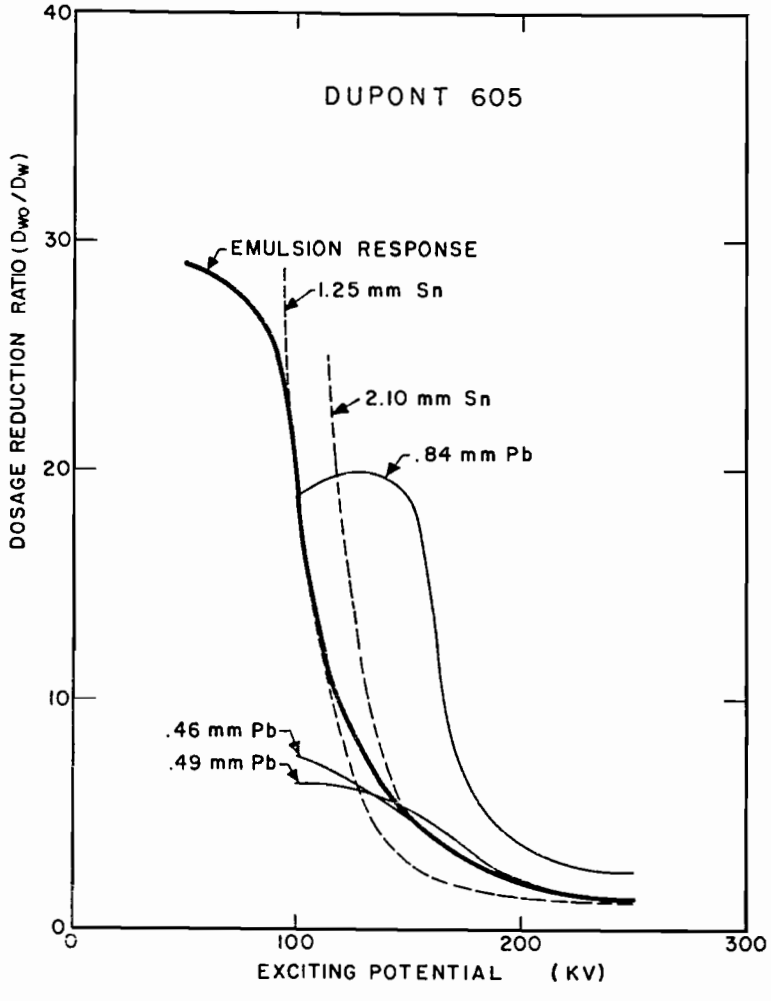

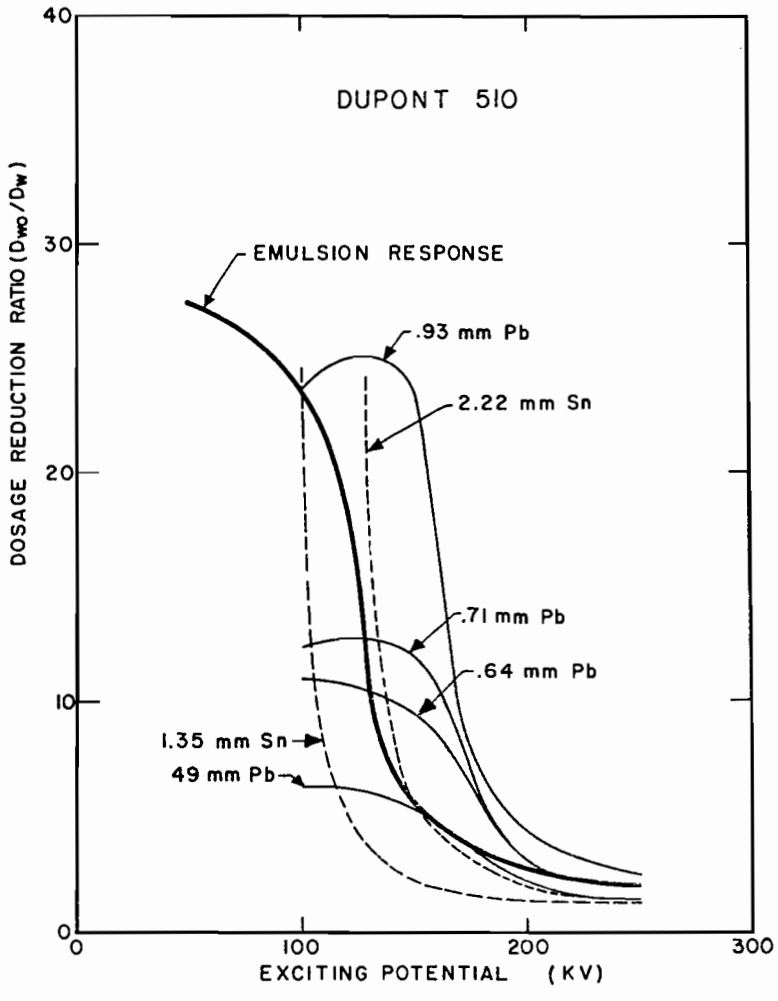

Fig. 3.9 Matching of Dosage Reductions and Du Pont Response Coefficients

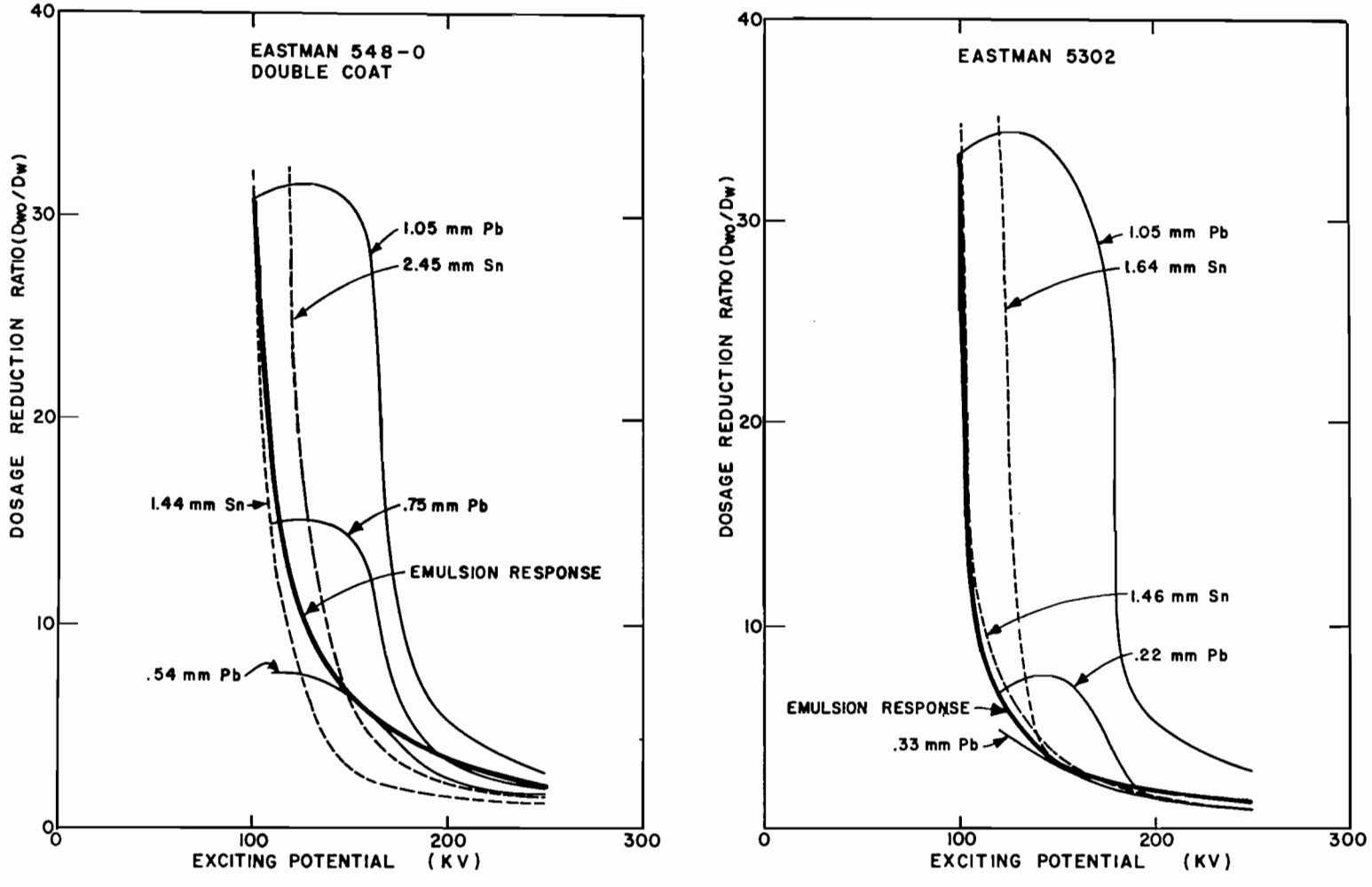

Fig. 3.10 Matching of Dosage Reductions and Eastman Response Coefficients

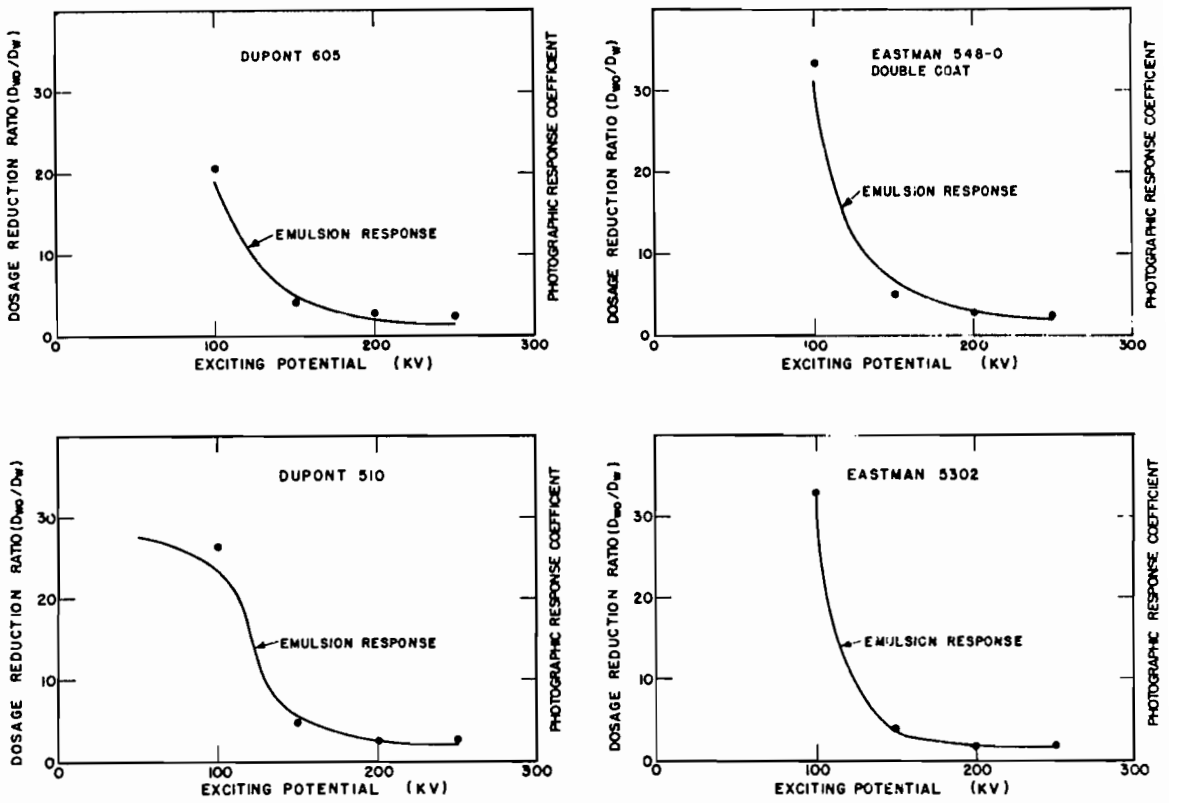

Fig. 3.11 Performance Expected of the Chosen Absorber Combinations. The solid lines represent the course of the response coefficients of the film emulsions. The points show the dosage reductions expected of the following absorber combinations: Du Pont 605, 1.25 mm of tin plus 0.1 mm of lead; Du Pont 510, 1.35 mm of tin plus 0.25 mm of lead; Eastman 548-0, 1.49 mm of tin plus 0.25 mm of lead; and Eastman 5302, 1.46 mm of tin.

[redacted]

TABLE 3.7 PER CENT INACCURACY IN DOSAGE INTERPRETATION IN THE RANGE FROM 35 TO 600 KEV

	Inaccuracy* (%)			
Kev	Du Pont 510	Du Pont 605	Eastman 5302	Eastman 548-0 (Double Coat)
35	−93	−93		
70	−33	−54	−69	−60
122	+6	−19	−47	−20
172	+24	+7	−25	−15
210	+10	+2	−23	−4
350	+7	0	−11	−2
600	0	0	0	0

*A minus sign signifies underreading, a plus sign, overreading.

REFERENCES

1. B. Kalmon, The Blackening Effect of Neutron and Gamma Radiation on Du Pont 552 and Eastman V-120 Film, Report ORNL-394, November 1949.
2. T. E. Shea, Jr., private communication.
3. Berthold and Glocker, Ueber die photographischen und ionometrischen Intensitaetsmessungen an Roentgenstrahlen verschiedener Wellenlaenge, Z. Physik, 31(1-4): 259-264 (1925).
4. G. E. Bell, The Photographic Action of X-rays, Brit. J. Radiology, 9: 578-605 (1936).
5. Tochilin et al., A Calibrated X-ray Film Badge Dosimeter, Naval Radiological Defense Laboratory, Report ADP-78.
6. R. Baker and L. R. Silverman, An Improved Film Badge Method for the Accurate Determination of Personnel Exposures, Report UCLA-53.
7. L. A. Pardue et al., Photographic Film as a Pocket Radiation Dosimeter, Argonne National Laboratory, U. S. Atomic Energy Commission, Report MDDC-1065.
8. L. J. Deal et al., Roentgen-ray Calibration of Photographic Film Exposure Meter, Am. J. Roentgenol. Radium Therapy, 59: 731-736 (1948).
9. H. A. Kramers, On the Theory of X-ray Absorption and of the Continuous X-ray Spectrum, Phil. Mag., [6] 46: 836-871 (1923).
10. Kulenkampff, Ueber das kontinuierliche Roentgenspektrum, Ann. Physik, 79: 548-596 (1922).

[redacted]

[redacted]

Chapter 4

Calibration Procedure

4.1 THE CALIBRATING RADIATION

4.1.1 Calibration Points

The photographic dosimeter was calibrated with the X radiation from a 10-mev betatron and from a 1.4-mev constant potential X-ray unit. The dosimeter was also checked at six points of lower radiation energies (see Sec. 3.3.3). The calibration was made against a Victoreen roentgen meter with equilibrium wall thickness, which in turn was calibrated against a standard free-air chamber. Since bakelite was the equilibrium material around the photographic emulsions, lucite, whose effective atomic number is close to that of bakelite, was chosen as the equilibrium material around the Victoreen thimble.

4.1.2 Dosage Rate

In the energy range between 30 and 210 kev, where the film sensitivity varies by as much as a factor of 10 with the spectrum of the exposing radiation, it was necessary to select the beam spectrum carefully and to specify it uniquely.

Although it is true that added filtration in the X-ray beam will make the X-ray spectrum more nearly monochromatic, it also reduces the dosage in the required energy range. The reduction of the dosage rate means increased exposure time for the calibration. A compromise was therefore required.

In the present work, a dosage of 0.025 roentgen per minute and milliampere at 1 meter distance from the target was considered acceptable.

4.1.3 Radiation Filters

The absorber combinations and absorber thicknesses used to obtain the specified radiation spectra from a constant potential X-ray machine were determined theoretically by considerations based again on the modification of a triangular X-ray spectrum by means of absorbers.

The method of selecting filter combinations for the various exciting potentials is best illustrated by means of an example. Figure 4.1 gives the differential dosages, dD/dE, at 250-kv exciting potentials behind a 2-mm lead filter, its modification when 1 mm of tin is added to the lead, and finally the differential dosages behind a filter consisting of 2.67 mm of lead and 1 mm of tin. The spectrum behind the lead filter shows clearly that lead was entirely ineffective below its absorption edge. A sufficiently thick tin filter had to be added in order to reduce the portion of the spectrum below the lead absorption edge and in this way to narrow the transmitted spectral band.

An experimental test of this lead-tin combination filter revealed that the half-value layer of the radiation which it passes is 3.3 mm of tin and the beam intensity is 0.049 roentgen per minute and milliampere at 1 meter, which is about twice the desired intensity. The graph of radiation quality (as measured by its half-value layer of tin) versus beam filtration (in tin thickness) at 250-kv exciting potential (Fig. 4.2) shows that the half-value layer of the originally selected filter (point A on curve) still lies in a region where the half-value layer varies appreciably with filter thickness. This is an expression of the fact that the radiation

[redacted]

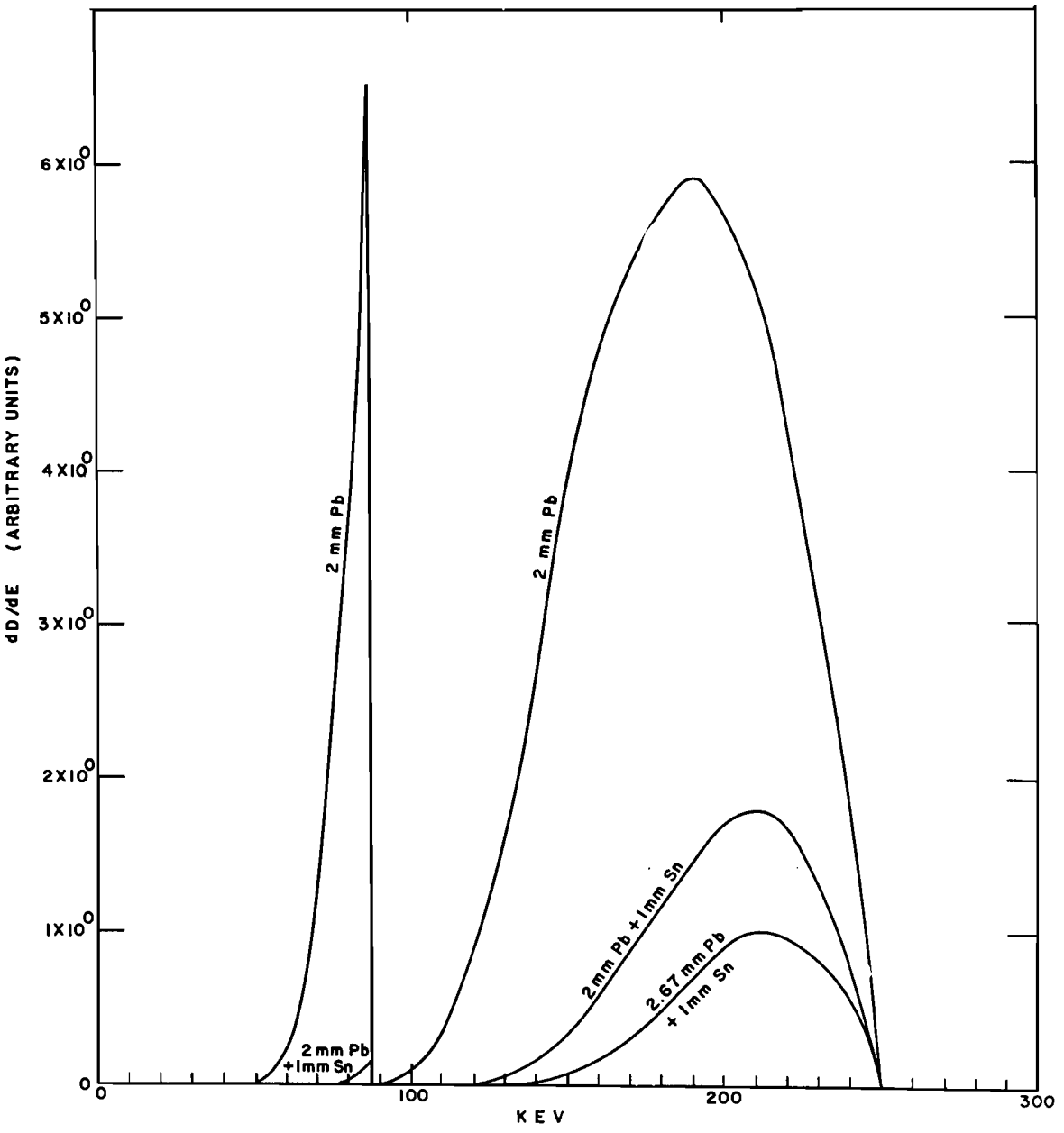

Fig. 4.1 Modification of 250-kv Radiation Spectrum by Means of Filters

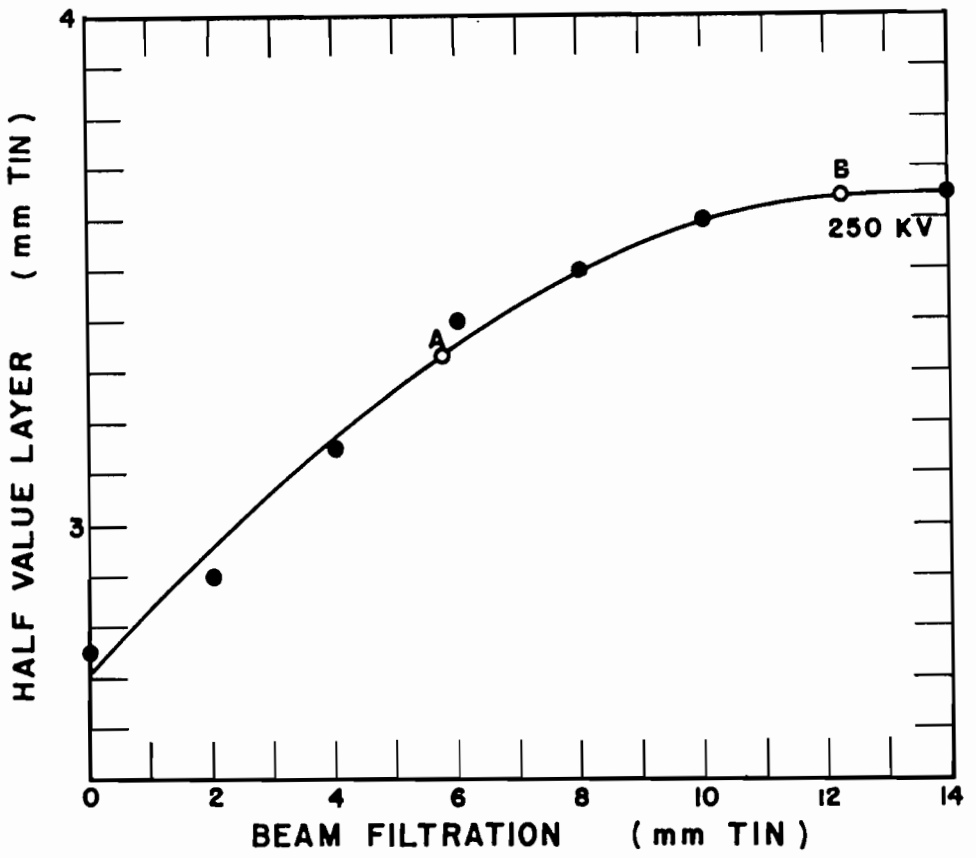

Fig. 4.2 Half-value Layer of X Radiation as Function of Beam Filtration Determined by Tin Absorption Measurements. Point A represents the performance of a composite filter of 2 mm of lead and 1 mm of tin; point B represents the performance of a composite filter of 2.67 mm of lead and 1 mm of tin.

passing through the filter is still highly heterochromatic.

The addition of another half-value layer of lead to the original filter combination produces a more adequate result (point B in Fig. 4.2). The new filter passes a radiation intensity of 0.025 roentgen per minute and milliampere at 1 meter, which is the desired output.

Similar reasoning led to filters for all other desired calibration potentials. Figure 4.3 shows the theoretical spectral distributions passed by the four calculated filters. In order to specify the beam quality in each case, a "spread" was defined as

$$W = \frac{(E_2^{1/2} - E_1^{1/2})E_{exc}}{E_p} \qquad (4.1)$$

where E_{exc} is the exciting energy, E_p is the energy of the intensity peak, and $E_2^{1/2} - E_1^{1/2}$ is the energy-band width at half the peak intensity.

Table 4.1 lists the characteristics of the selected filtrations. It shows their theoretical spread, W, and the experimentally determined radiation intensity which passes through them. The experimentally determined half-value layers and effective potentials of the resulting X-ray beams as well as their theoretical intensity peaks are included for comparison.

If lower intensities are permissible, the spreads may be decreased by adding more filter material. In the case of combination filters, only the thickness of the high atomic number element has to be increased.

4.2 PROCESSING

The photographic film density is influenced materially by the type of processing. Once a routine is established, it has to be strictly adhered to. The following discussion deals with the successive phases in the processing of films for the Greenhouse dosimeters.

4.2.1 Developing

The choice of the developing agent was the most decisive step for the entire processing sequence. It determined the useful exposure range of the photographic emulsions as well as their contrast. Figure 4.4 illustrates for a series of developing times the differences between the fast Eastman and Ansco X-ray developers and the fine-grain Ansco Reprodol developer, all used at a temperature of 20 ± 0.1°C. The curves represent graphs of densities versus the logarithm of the exposures received by Ansco Reprolith orthochromatic films. The set of films developed in the X-ray developers received exposures identical with the ones that were developed in the fine-grain developer. But the densities reached in the X-ray developers at any given exposure were almost three times those in fine-grain developer. It is thus possible to extend the useful range of a photographic emulsion by using both a fast and a slow developer. This was, however, considered inexpedient for the present test, and the Reprodol developer was therefore eliminated.

An inspection of the family of curves obtained with the Eastman X-ray developer showed that at a developing time of 5 min one is close to the maximum density achievable at a given exposure, whereas the density is still increasing markedly after a 5-min development in the Ansco X-ray developer. On the basis of these results it was decided to use the Eastman developer and to develop all emulsions for 5 min. It was then adequate to time the development by means of one of the spring-type photographic timers. Possible inaccuracies introduced by fluctuations in the developing temperature could be eliminated by the use of processing corrections.*

According to Wilsey,[1] a solution like the Eastman X-ray developer shows signs of exhaustion after the development of two 8- by 10-in. X-ray films per liter. It was decided to discard rather than to replenish the developing solution before it showed signs of exhaustion. At Greenhouse, approximately 300 dental films were developed simultaneously. The emulsion area of 300 dental films is approximately 1320 sq in. (considering both film sides). Since 5 gal of developing solution was allowed for each 300 films, an area of 6400 sq in. or at least 1200 films could be developed in the same solution without exhausting it noticeably. It was decided, however, to allow for a larger safety margin and to discard the solutions after the development of only 600 films per 5 gal. The

* Experiments showed that a temperature fluctuation of ±0.25°C introduces an error in the dosage interpretation of approximately 5 per cent.

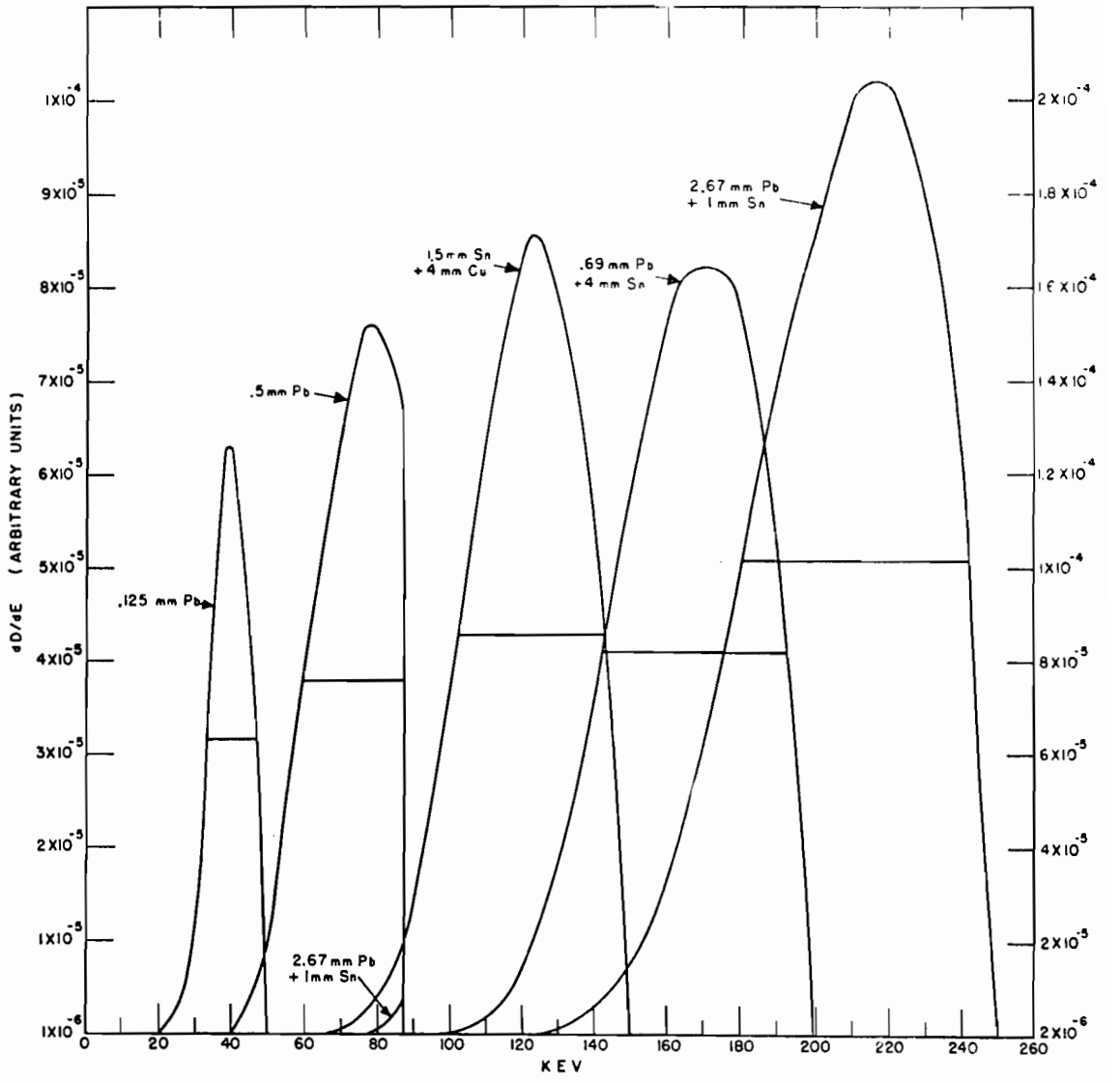

Fig. 4.3 Theoretical Spectral Distributions of the Calibrating Radiations. The ordinate on the left refers to all but the 100-kv spectrum, for which the ordinate on the right should be used.

TABLE 4.1 CHARACTERISTICS OF THE SELECTED FILTRATIONS

Filter	Kv	Spread	Half-value Layer (mm Sn)	Theoretical Intensity Peak	Experimentally Determined Effective Potential
2.67 mm Pb 1 mm Sn	250	42.1	3.64	216.5	210
0.25 mm Pb 4 mm Sn	200	64.7	2.19	170	172
1.53 mm Sn 4 mm Cu	150	50	1.01	123	122
0.53 mm Pb	100	35.5	0.33	77.5	70
0.125 mm Pb	50	17.5	0.08	35.5	

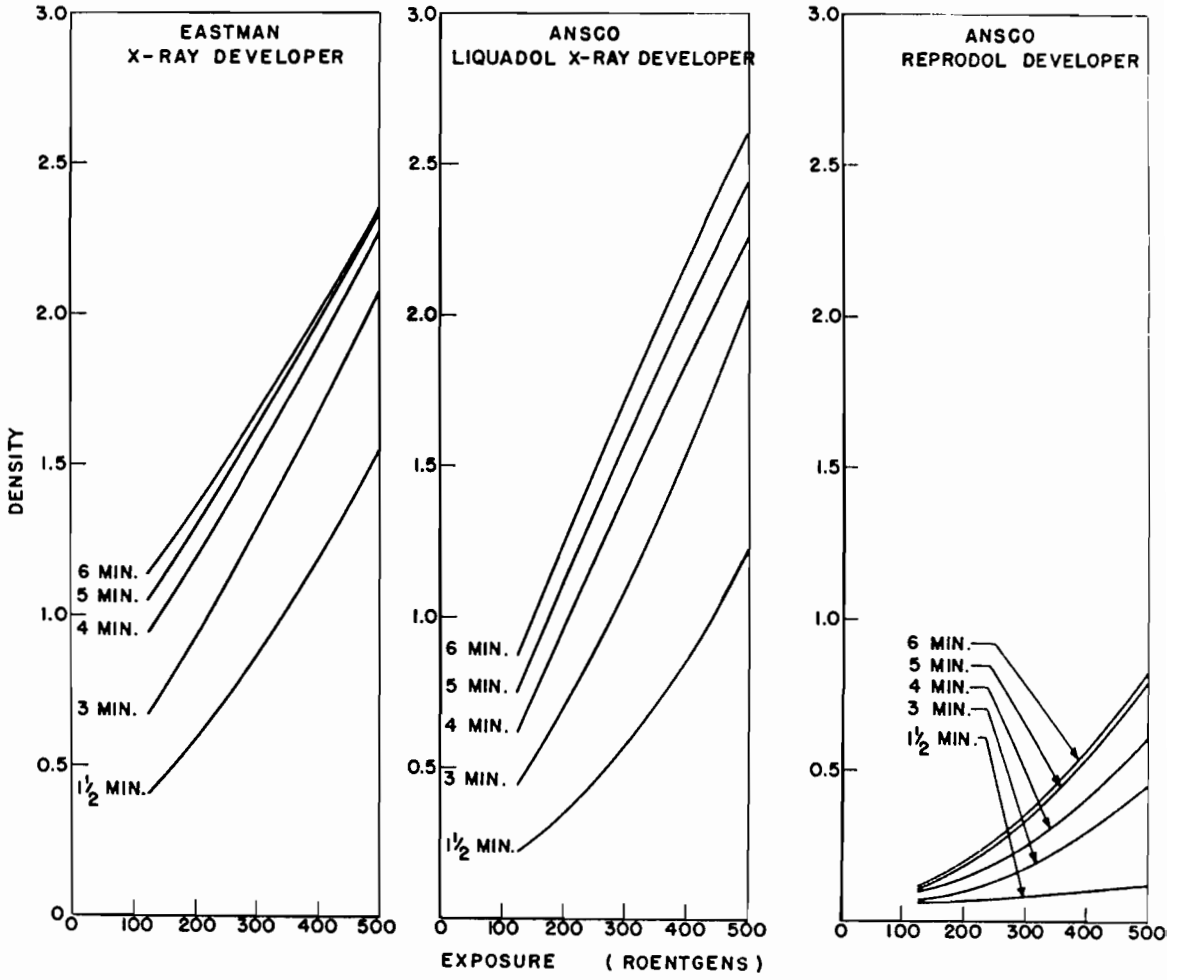

Fig. 4.4 Influence of Choice of Developer on Final Film Density

consistency of the Greenhouse developing process was checked by means of sets of Du Pont 510 films exposed to a known dosage and developed along with the unknowns.

The film racks used at Greenhouse were similar to the ones employed in the processing of the dosimeter calibration films. The racks were designed to hold approximately 300 dental-size photographic films between two strips of corrugated stainless steel, with five sections, each holding 60 films, stacked on top of each other.

It is general practice to agitate photographic materials during development in order to ensure uniform emulsion density. But the more individual films there are to be developed at a time, the harder it is to agitate them effectively without introducing disturbing currents in the developing solution.

The Greenhouse film racks were tested in their performance both with and without agitation, when loaded with heavily exposed films. The agitation consisted in a vertical motion of the entire film racks parallel to the film surfaces with a speed of about 15 in. per minute. Superimposed on this motion was a rocking motion which tilted the film surfaces through approximately 30 degrees to either side of the direction of the vertical motion.

When the films were developed without agitation, the developing solution was thoroughly stirred immediately before use.

The results of this test were as follows: The average density of the agitated films was about 5½ per cent above the density without agitation, but the maximum variation in density on any single film was 6 per cent with and only 4 per cent without agitation. The agitating system thus proved effective in removing the used developing solution from the film surface, but it also seemed to introduce currents which streaked the emulsion. However, while the film-to-film density variations with agitation were slightly larger than without, they were entirely random. When the films were stationary during development there was a slight gradient noticeable on each film and a tendency to underdevelop the lower portion of the films. There was also a vertical gradient from section to section, resulting in a difference of about 2 per cent between the average film density of the second section from the bottom compared with the top and bottom sections. It was decided to use the film racks without agitation and to correct for possible variation in development by means of control films of known exposure.

4.2.2 Fixing

In order to stop the developing action immediately after removal of the photographic materials from the developing solution, the films were rinsed for about 20 sec in an acid stop bath. This prevented streaking of the emulsions during the stationary fixing. The stable Eastman X-ray fixing bath was selected as adequate. Since films should be fixed at least twice as long as it takes them to clear, the standard method was adopted to fix all films for 10 min and to discard the solution when the clearing time approached 5 min.

4.2.3 Washing and Drying

The films were washed in running water for a period of about 15 min and dried in a stream of cool air. This procedure ensured good keeping quality over a period of years. The temperature of the wash water was kept close to the processing temperature in order to avoid stresses on the wet emulsions. Drying was facilitated by placing the film material into a water bath containing a wetting agent for about 3 to 5 min after the regular wash period. Since the mode of drying influences film density, the drying procedure was standardized by the use of similar commercial dryers for the calibration work at the National Bureau of Standards and at Greenhouse.

4.3 STANDARDIZED FILM DENSITOMETRY

The photographic transmission densities were read on a calibrated photoelectric densitometer with a range up to 6. The high density range extended the useful exposure range of each film emulsion. If there were consistent differences of 5 per cent or more between the densities of the films of known exposure and films of unknown exposure when they were developed together, the densities of the films of unknown exposure were corrected. Although, for best accuracy, controls should be supplied

[redacted]

for all four film types for density regions in which density may be roughly considered a linear function of exposure, this was considered superfluous for Operation Greenhouse. The reason was that the inaccuracies due to development were well within the over-all inaccuracy of the dosimeter. Controls were therefore supplied only at one convenient density for the Du Pont 510 film. The ratio of expected control film density to actual control film density was used as the density correction factor.

REFERENCE

1. R. B. Wilsey, The Photographic Photometry of Roentgen Rays, Am. J. Roentgenol. Radium Therapy, 32(6): 791 (1935).

[redacted]

Chapter 5

Calibration Results

This chapter gives a discussion of the set of calibration curves which was used in the interpretation of the Greenhouse exposures. The data are presented in Figs. 5.1 through 5.5 in form of photographic density-versus-exposure graphs. Figures 5.1, 5.2, and 5.3 represent the calibration results on the films in the bakelite-tin-lead badges for different radiation energies, and Figs. 5.4 and 5.5 show the results of a comparison calibration of four of the five films which was done without badge at an effective radiation energy of 600 kev only.

The calibrations with and without badge are very similar for all four emulsions; the differences are of the order of 10 per cent, maximally, and are usually so small as to lie within the limits of errors inherent in the photographic method. The fact that some films are more sensitive with and some without the badge may be due to a difference in their electron sensitivities.

The film-badge calibration curves of the Du Pont 510, Du Pont 605, Eastman 5302, and Eastman 548-0, double coat, are for 600-kev effective radiation energy and for the radiation from a 10-mev betatron. The low-energy points which were the basis for Table 3.7 are included for comparison. No work was done on Eastman 548-0, single coat, with any radiation other than 0.6 mev. It can be inferred, however, from previous work with this emulsion that its change of sensitivity with energy is similar to that of the Eastman 548-0 double-coat emulsion.

As shown in Figs. 5.1 and 5.2, the sensitivity of the four films exposed to radiation from the 10-mev betatron is such that an interpretation of dose from the 0.6-mev calibration curve will be within ±7 per cent of an interpretation from the betatron calibration curve.

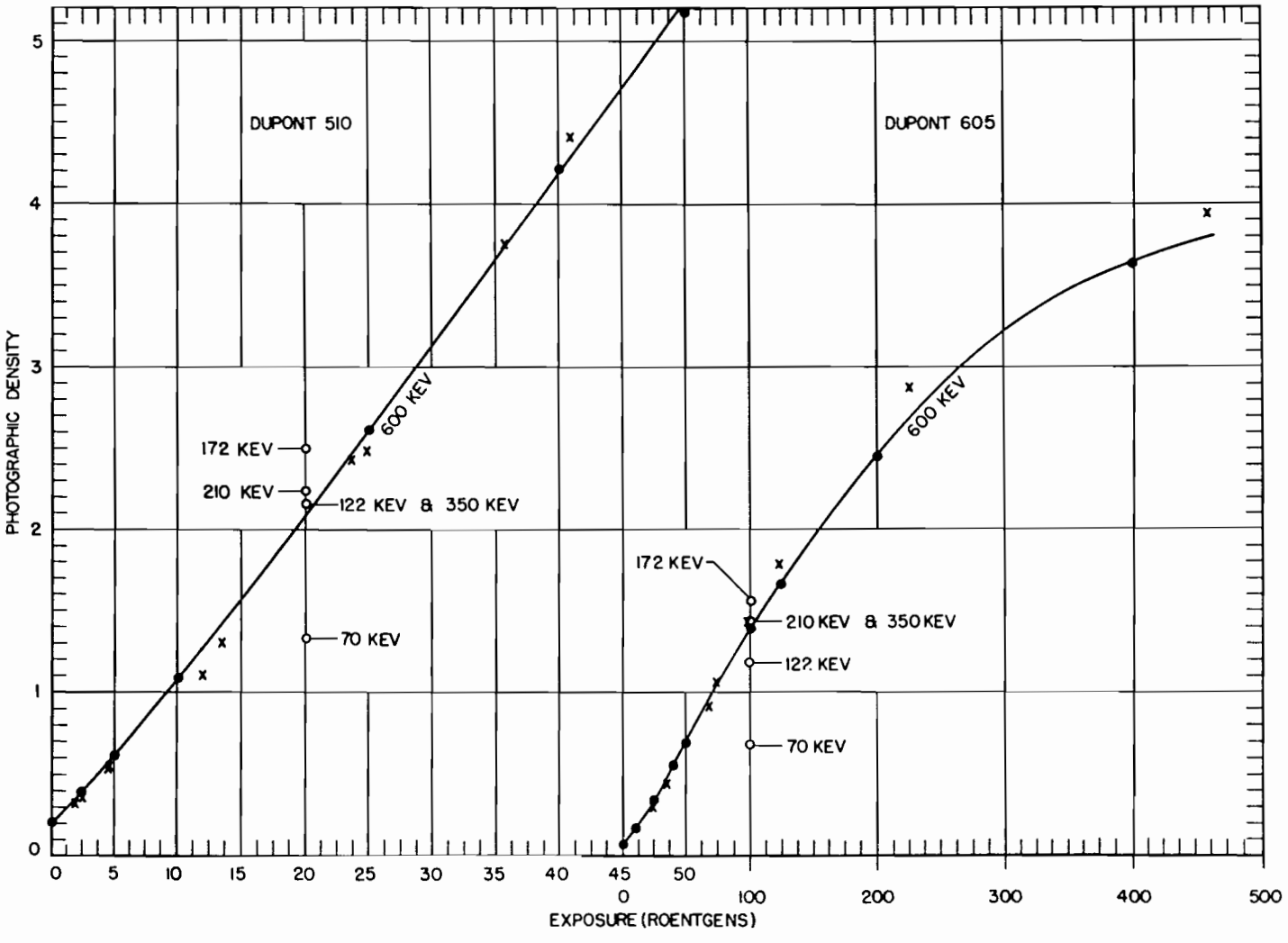

Fig. 5.1 Calibration of Absorber Film Badge; Exposure Range from 1 to 500 Roentgens. The points represent the calibration results at 0.6 mev; the crosses represent the calibration results obtained with a 10-mev betatron.

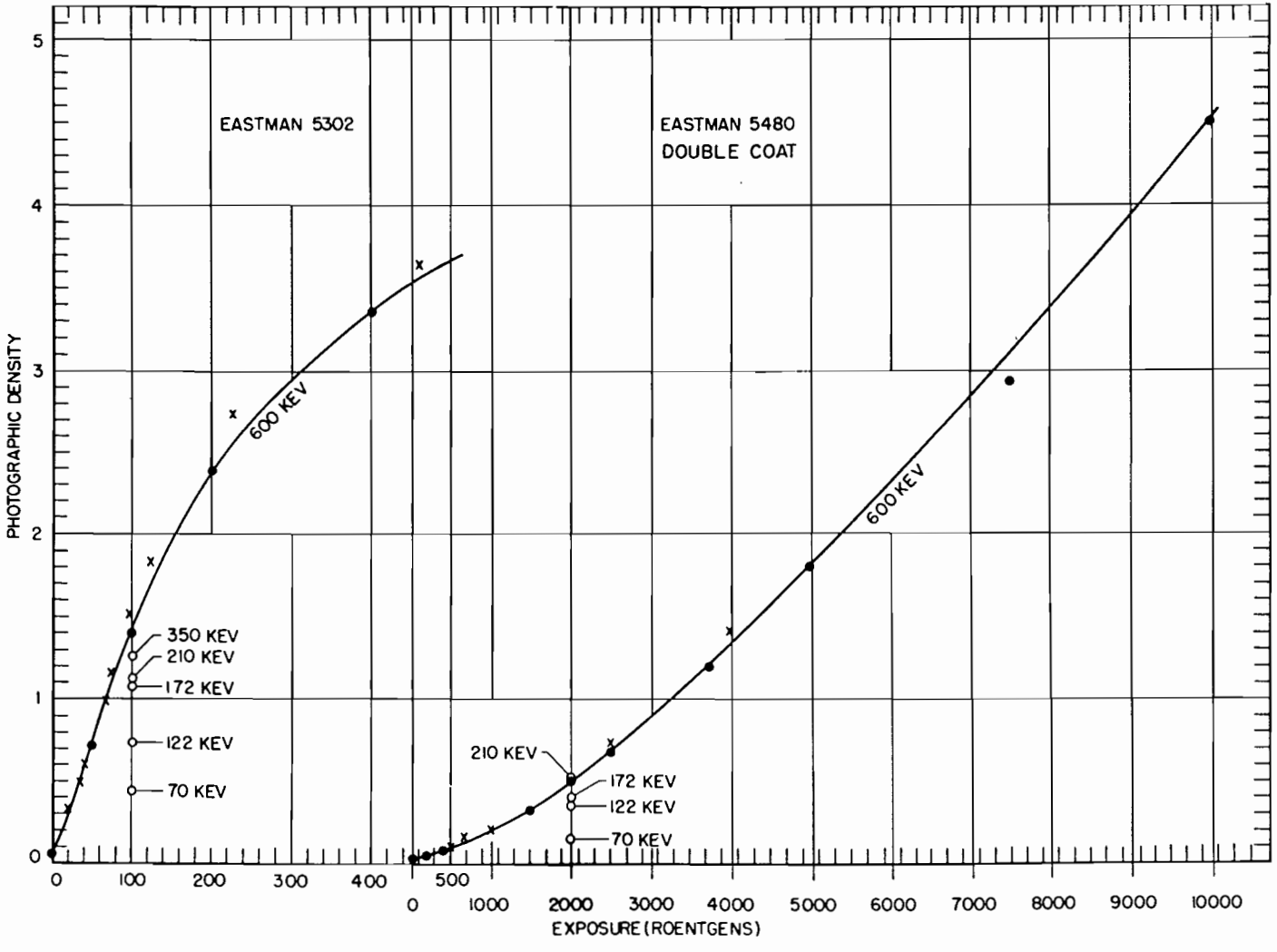

Fig. 5.2 Calibration of Absorber Film Badge; Exposure Range from 20 to 10,000 Roentgens. The points represent the calibration results at 0.6 mev; the crosses represent the calibration results obtained with a 10-mev betatron.

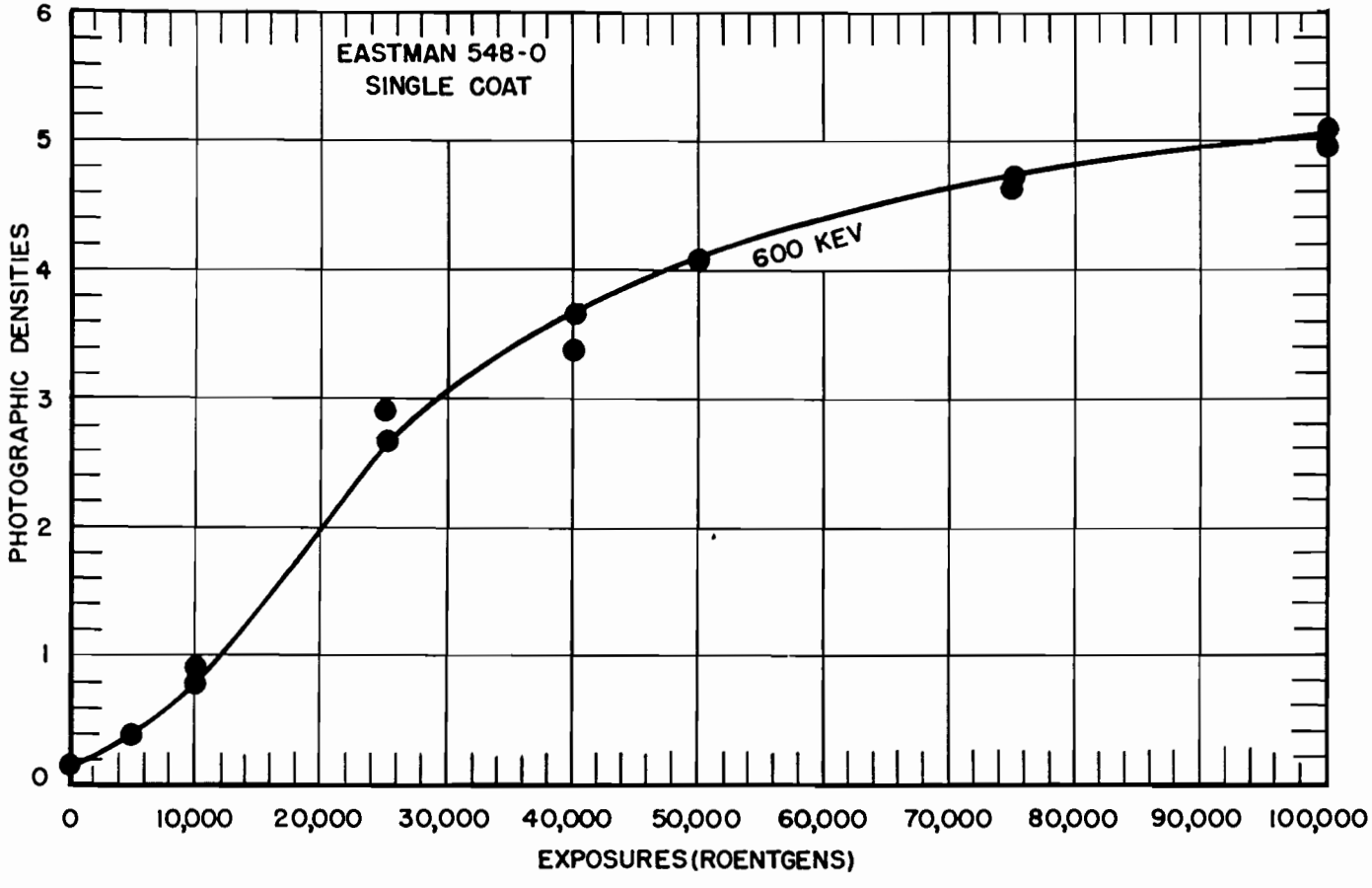

Fig. 5.3 Calibration of Absorber Film Badge; Exposure Range from 5000 to 100,000 Roentgens

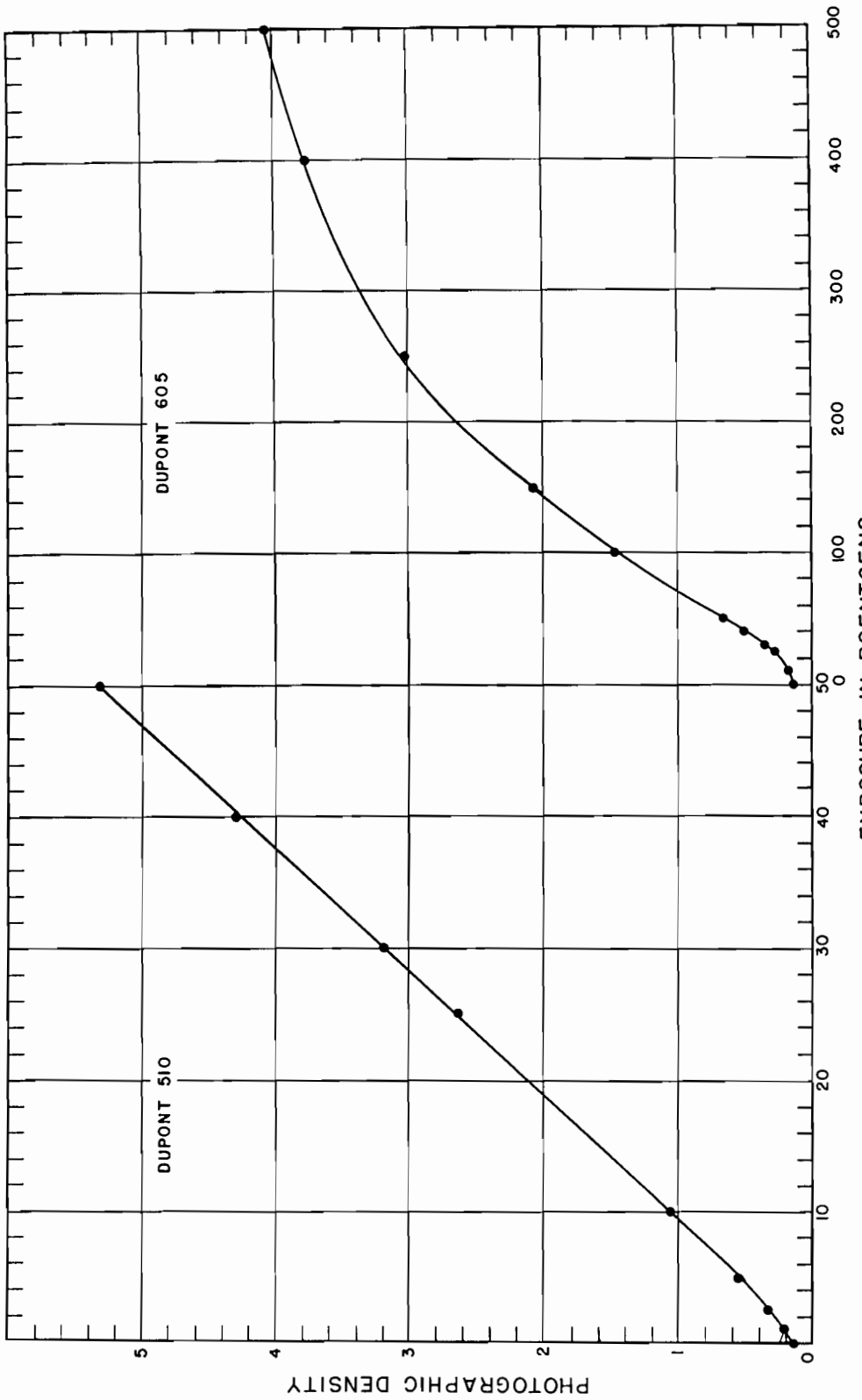

Fig. 5.4 Calibration of Bare Film Packets; Exposure Range from 1 to 500 Roentgens

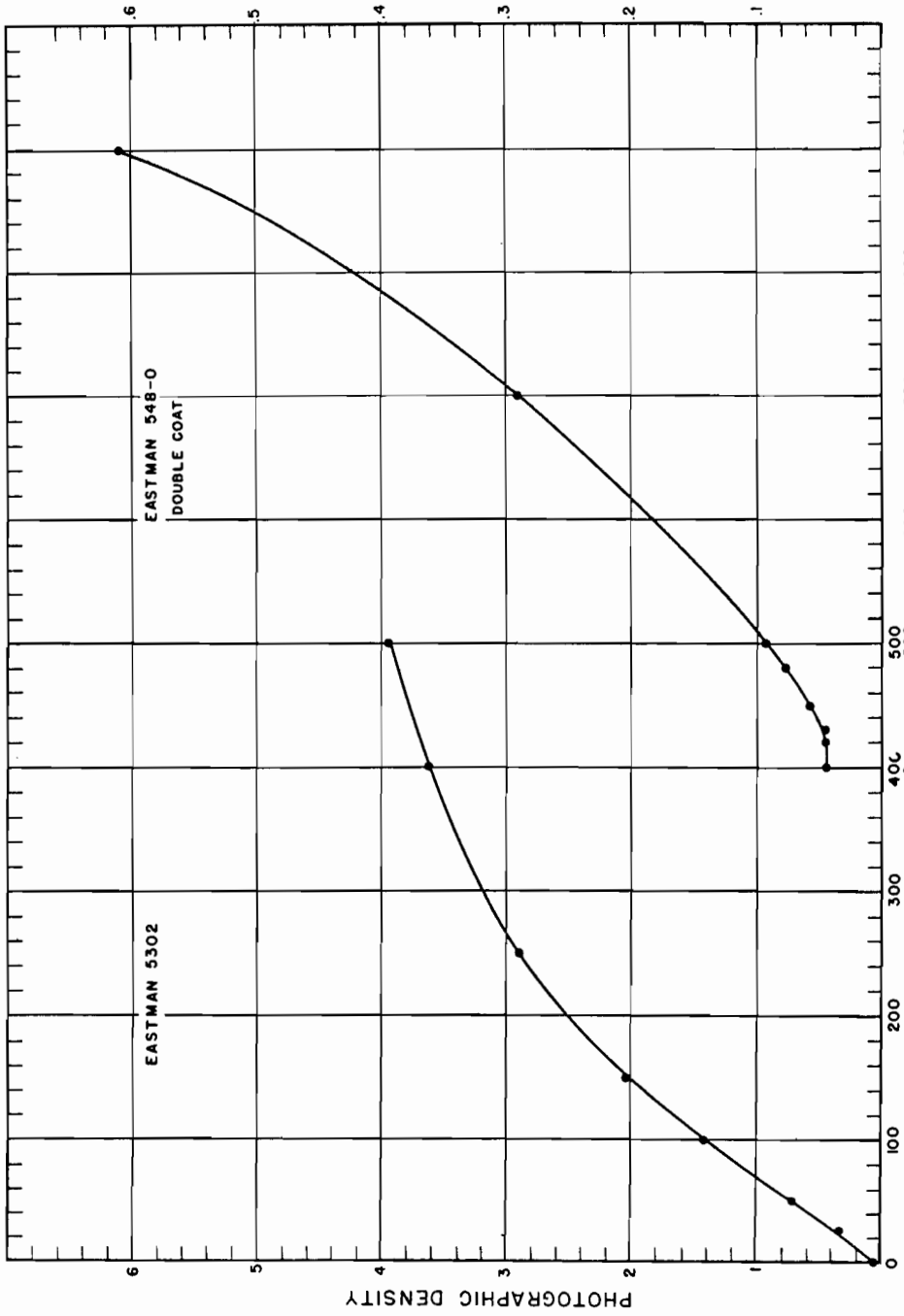

Fig. 5.5 Calibration of Bare Film Packets; Exposure Range from 25 to 2500 Roentgens

Chapter 6

Results of Field Measurements

6.1 INTRODUCTION

The Greenhouse film program consisted of four phases:

a. Determination of total dose versus distance.
b. Determination of time dependence of dose rate at various distances by use of film traps.
c. Measurement of total dose at various sheltered positions.
d. Distribution and processing of films to be used as total-dose monitors in other programs.

6.1.1 Accuracy of Results

The over-all accuracy of the dose determination may be estimated by reference to Chap. 5. It is seen, however, that some knowledge of the spectral distribution of the radiation is necessary. A rough estimate of an "effective" energy of the gamma radiation may be obtained from the dose-distance information (see Fig. 6.3), where it may be seen that the effective broad-beam absorption coefficient is 3.08×10^{-5} cm^{-1} at those positions where the dose is less than 10,000 roentgens. Since the build-up factor behaves very closely as $x^{1.25}$ after several mean free paths, for energies such that the Compton effect predominates, the narrow-beam absorption coefficients, μ_{NB}, may be estimated from

$$I = I_0 \frac{\exp(-\mu_{NB} x)}{x^2} x^{1.25} \qquad (6.1)$$

This yields $\mu_{NB} = 3.85 \times 10^{-5}$ cm^{-1}, which corresponds to a gamma-ray energy of approximately 4 mev.

It may be said, in general, that at large distances from the source the attenuation coefficient is determined by the most penetrating radiation present in quantity in the source. However, the amount of low-energy radiation is determined by the transmitting medium rather than the source. Thus, in air, low-energy radiation[1] may be expected down to about 60 kev. The 4-mev figure derived above represents an effective upper limit to the gamma-ray energy. The use of the word effective implies that there may be higher energy components present but the spectrum falls off at such a rate that they do not make appreciable contribution to the dose.

This rather crude determination of effective energy coupled with the estimate of the spectrum at points much closer to zero (see Greenhouse Report, Annex 1.2, Part I) would indicate that the radiation actually detected by the badges in the field is somewhat like the radiation from the 10-mev betatron. The discussion of Greenhouse Report, Annex 1.2, Part I, would indicate, however, that the spectrum observed in the field would have relatively more low-energy content than would the 10-mev betatron. Thus the badges were actually exposed (in the field) to a spectrum which might be considered a cross between the 10-mev betatron radiation and 1400-kev (max.) X rays which were used to calibrate the films. Thus the value of ±7 per cent found in Chap. 5 is considered applicable.

In addition to the systematic error just discussed, random errors will arise in processing and densitometering the film. Prior to their exposure in the field, films used in total-dose gamma-ray measurements at Operation Greenhouse were stored at a temperature of about 14°C except while in transit. Even then they

were under surveillance to see that they were not unduly damaged by either heat or radioactive materials. In order to achieve sufficient dosage range coverage, it was necessary to order films from both Eastman Kodak and Du Pont. It required about three months for delivery of the Eastman Kodak films, but the Du Pont films were delivered within a few days of the receipt of order. Since the films were to be used at about the time of their expiration date, there was some question about whether or not they should be used. As a precautionary measure, a new order for Du Pont films was placed during the latter part of February 1951. The new films were held in reserve at the test site in case it became necessary to use them. However, upon exposure of the original films to dosages of 20, 30, and 50 roentgens of radium gamma rays at the test site, it was found that the densities thus produced agreed with the exposures within 5 per cent, according to calibration curves obtained several months previously for these films on 600-kev X rays. Furthermore, the background densities of the films agreed within 0.01 density unit of those previously obtained at the National Bureau of Standards Radiation Laboratory in Washington. Therefore the original Du Pont films were used in the tests.

A set of control films was maintained as a check on processing. These consisted of Du Pont films that had been exposed to X rays so that their densities after processing ranged from about 1.30 to 1.35. Several of these were developed after the mixing of each new batch of processing solutions to avoid the possibility of ruining films by solutions that might have been improperly mixed or which might have contained ingredients of the wrong strength. Furthermore, an entire hanger was loaded with these films and processed at the test site. It was thus determined that there was no observable dependence of density upon positioning either for films within a given tray or for various levels of trays within a hanger. Throughout the entire processing of films, one control film was developed in each tray as a further check on processing uniformity. Fresh developer was mixed to avoid noticeable change in its strength after each 2100 films were processed in a 15-gal tank of developer. The timer clocks were checked before usage and observed to be accurate within 2 sec out of 5 min. Two clocks were used simultaneously for each development since the clocks were regular darkroom clocks and therefore not always dependable. It is well that this precaution was taken because during one of the runs a clock did fail. The time required to remove a hanger from the developer and place it in the stop bath was about 5 sec. Since development is nearly complete after 5 min in the developer that was used, the timing error was a second order effect only. The mercury thermoregulator was set to maintain the temperature of the solutions at 19.85°C. When a hanger of six trays maintained at room temperature was inserted, its thermal energy caused the temperature of the developer within the trays to rise 0.10 to 0.15°C and remain that way for the most part throughout the developing process since no agitation was used. To determine the magnitude of the temperature dependence, a set of control films was run at the test site at various temperatures. These showed about 0.5 per cent change for a temperature variation of 0.10°C in the vicinity of 20°C. In consideration of this and all other errors inherent in the processing, it is believed that the over-all error in processing was 1 per cent.

In contrast with this are the much larger errors produced in densitometer readings and by the variations in density across individual films. For example, probable errors in densitometer readings were roughly as follows: 0.01 density unit for the density range 0 to 0.2, 0.02 for the range 0.2 to 3.0, and 0.03 for the range 3.0 to 6.0. These correspond to probable densitometer errors in dosage determination on the Du Pont 510 film of 5 per cent for the 5-roentgen reading, 3 per cent for 10 roentgens, 1 per cent for 20 roentgens, and 1 per cent for 50 roentgens. Similarly, probable errors caused by uncertainties in densitometer readings on the Du Pont 605 and Eastman 5302 films were 4 per cent for the 50-roentgen reading, 2 per cent for 700 roentgens, and 6 per cent for 1000 roentgens. Also, for the Eastman 548-0 double-coat film, the readings were 6 per cent for 500 roentgens, 5 per cent for 700 roentgens, 5 per cent for 1000 roentgens, 3 per cent for 2000 roentgens, and 1 per cent for 5000 roentgens.

Variations in density readings in individual films caused uncertainties comparable with those inherent in the densitometer process. In particular, the average percentage variations

in dosage measurement as observed for four readings across each film usually ranged from 2 to 6 per cent of the total dosage. These variations were independent of the type of film used and of the positions where they happened to fall on the H and D curves. Furthermore, the variations in densities across individual control films were uniformly within 1 per cent. Clearly, therefore, a large part of the uncertainty inherent in the film-badge method resulted from variations in electronic flux or energy dissipation across individual films. It is not evident whether the badge design was at fault or local scattering conditions surrounding the badges were largely responsible.

Regarding the random error of the film-badge interpretation, it is thus believed that the probable error is about 7 per cent. When combined with the calibration error, ±7 per cent, this gives an over-all probable error of about 10 per cent.

6.2 PHYSICAL SETUP

The film badge in various stages of assembly is shown in Fig. 6.1. The outermost wrapping is a brown paper bag. For total-dose measurements, four or five badges were taped to a pipe which extended about a foot out of the ground. Such a pipe is barely visible in Fig. 6.2, just to the right of the jeep wheel.

Sail film was used for the longer time exposures. A typical arrangement may be seen at the right of Fig. 6.2. The film was suspended near the top of a pipe by a rod until blast time. The blast, acting on a plywood sail connected to the rod, pulled the rod out of the pipe. The film then dropped into the bottom of the pipe which extended below the ground. Those films therefore received exposures only until the blast wave arrived.

For the shorter time exposures, the long (13-ft) drop pipes were used. About 5 ft of pipe extended below ground. A string of 15 badges was suspended inside the pipe, with the upper end of the string tied around the outside of the top of the pipe for support. A blast cap was attached to the string and was set off at zero time by an EG&G blue box. Exposure times ranged from about 0.1 to 0.7 sec. A typical tall drop pipe may be seen in the center of Fig. 6.2.

6.3 TOTAL DOSE VERSUS DISTANCE — RESULTS

The total-dose film packets were fastened, at about 8 in. above ground level, to $2\frac{1}{2}$-in. pipes which were driven into the ground. The number of badges attached to a pipe varied between three and five. The results for the four shots are summarized in Figs. 6.3 and 6.4. The effective narrow-beam absorption coefficient has already been determined in Sec. 6.1.1.

In order to determine whether the neutron flux made a sizeable contribution to the reading on the film, additional badges were installed inside lead houses, with walls $6\frac{3}{4}$ in. thick, at various distances. The readings on these films are indicated in Fig. 6.3. Since the attenuation of thermal neutrons in this thickness of lead has been determined* to be not quite a factor of 2, these lower curves in Fig. 6.3 indicate that the neutron contribution to the upper curves is negligible.

6.4 FILM-TRAP MEASUREMENTS— RESULTS

The readings on those films whose drops were initiated by the blast are shown in Fig. 6.5. It should be remembered that the various points represent different distances and shots, so that the degree of correlation to be expected is not immediately obvious.

Figure 6.6 contains the results obtained from the films in the tall pipes. Again, it should be remembered that these pipes were at different distances from ground zero.

6.5 DOSE MEASUREMENTS IN BUILDING 311

Figures 6.7, 6.8, and 6.9 are scale drawings of three levels in Building 311 on Engebi. The numbers are total doses, in roentgens, as measured by film dosimeters. Figures 6.10, 6.11, and 6.12 are graphs of dose versus distance from the front wall. The dose is seen to fall off much more rapidly than could be accounted for by inverse square or atmospheric absorption, and it actually corresponds to an

* This measurement was made on the thermal neutron column of the Brookhaven pile.

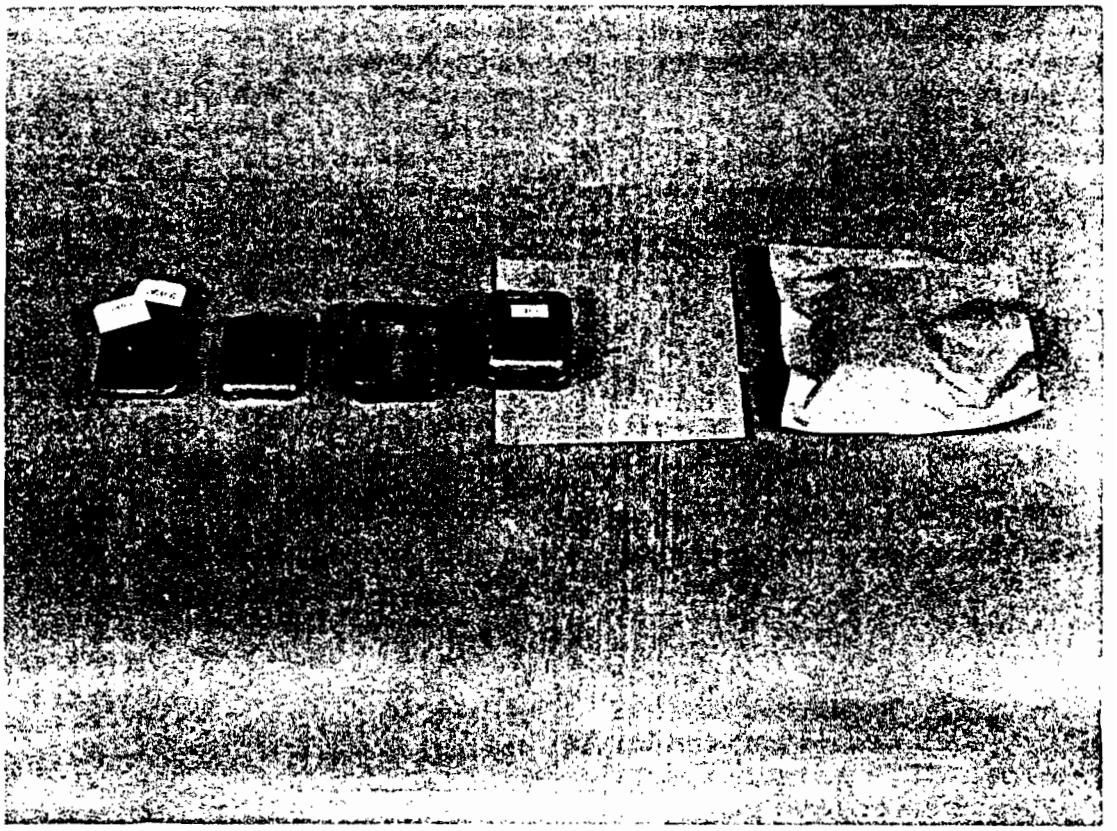

Fig. 6.1 Film Badge in Various Stages of Assembly

Fig. 6.2 Typical Setup of Total-dose, Sail, and Drop Film

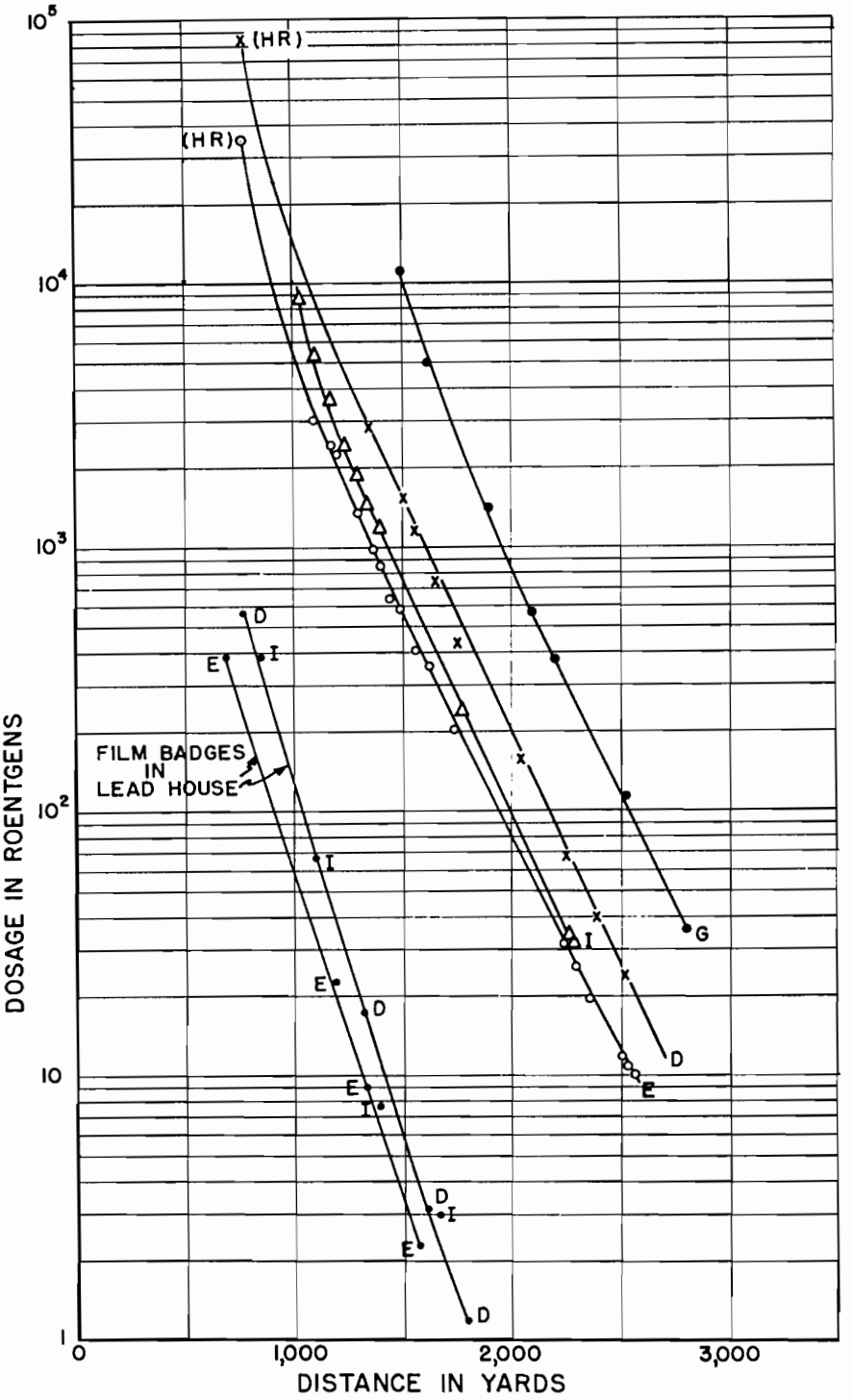

Fig. 6.3 Total Dose versus Distance for the Four Greenhouse Shots. The walls of the lead houses were $6\frac{3}{4}$ in. thick. Curves are labeled D for Dog shot, E for Easy shot, G for George shot, and I for Item shot.

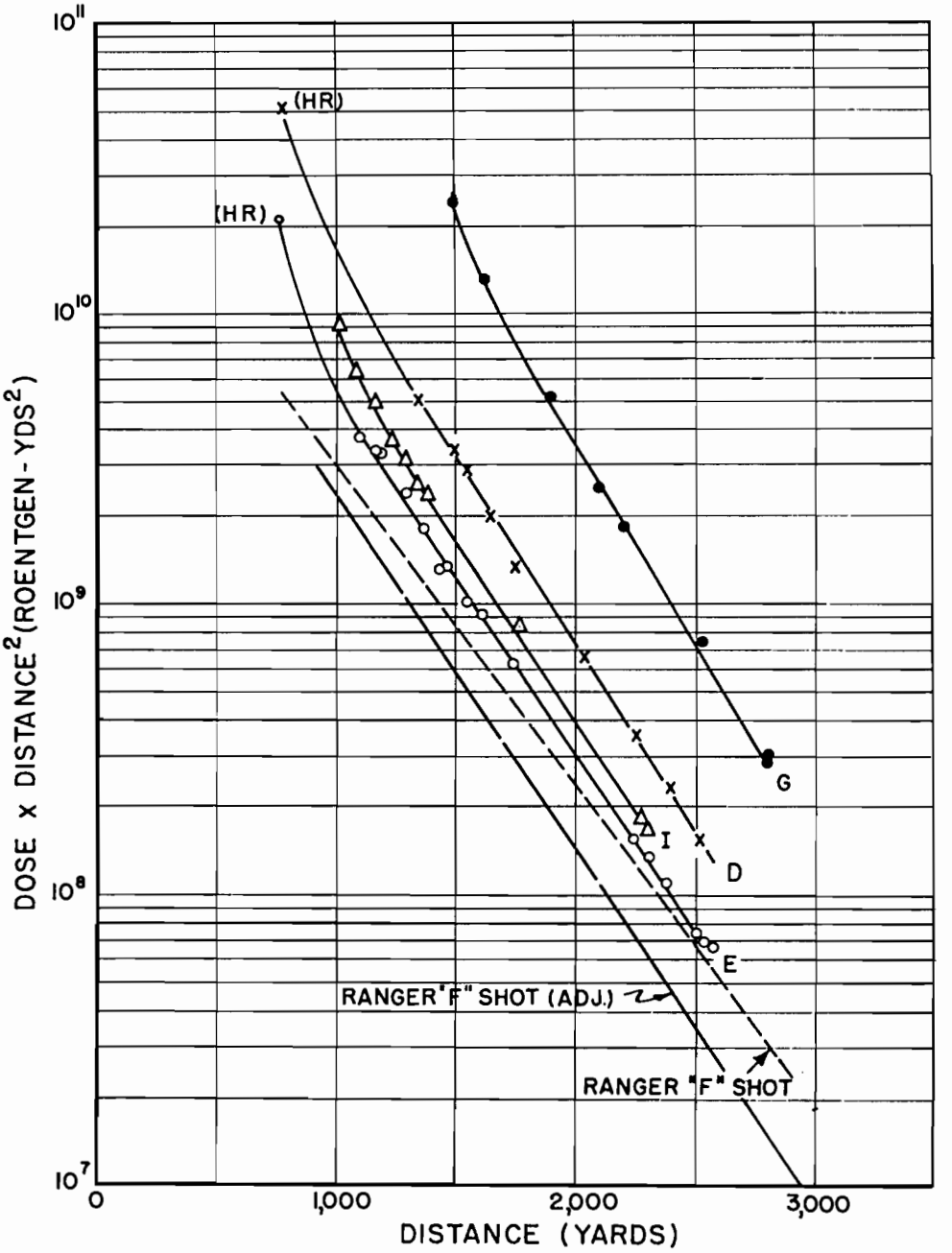

Fig. 6.4 Total Dose Times Distance Squared versus Distance for the Four Greenhouse Shots. The adjustment of the Ranger "F" shot data was achieved by correcting the original data for the different densities of air in the two tests.

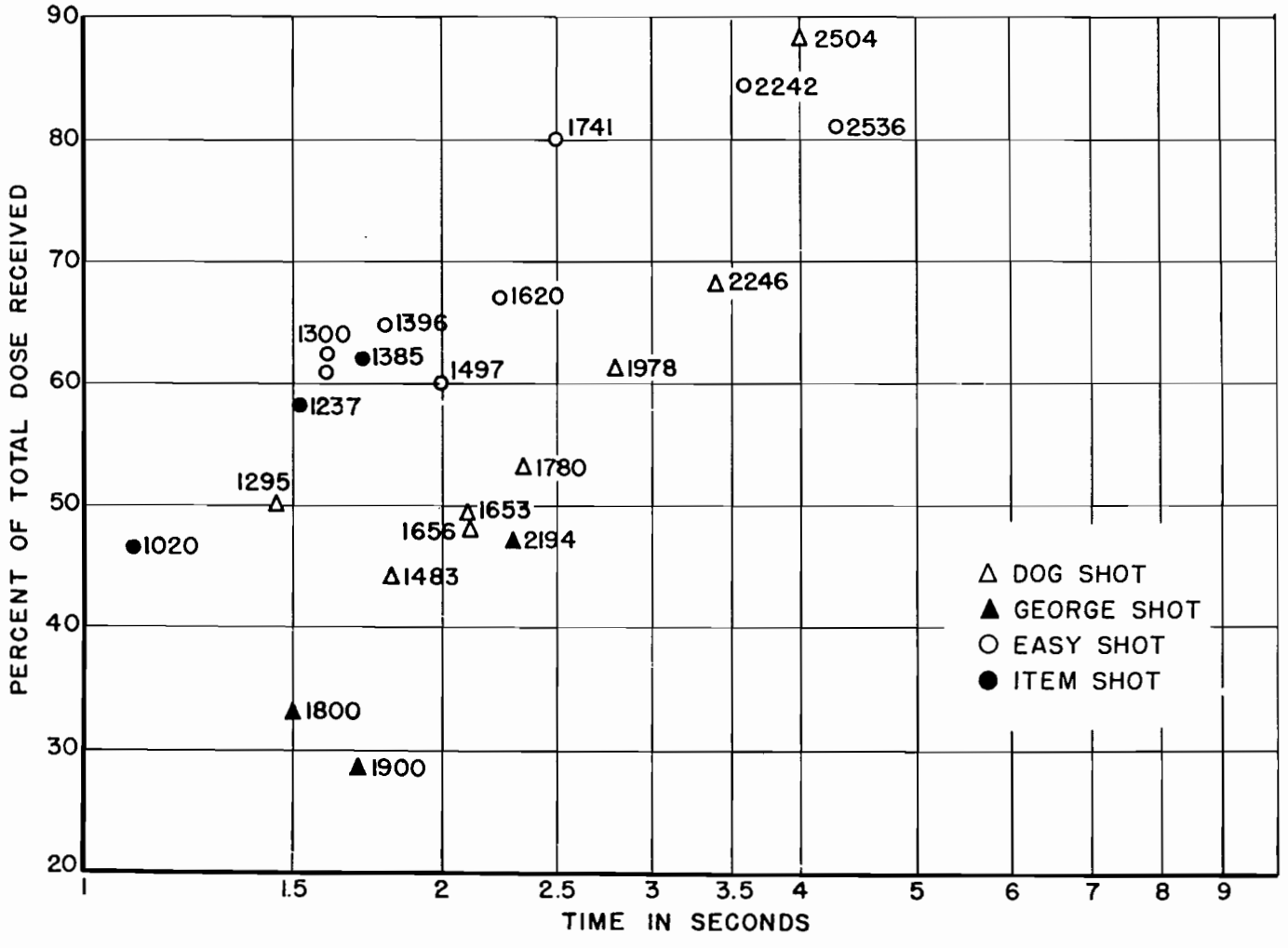

Fig. 6.5 Percentage of Film Dose Received at Various Times—Blast Initiated Film Drops. The number above each datum is the distance of the pipe from ground zero in yards.

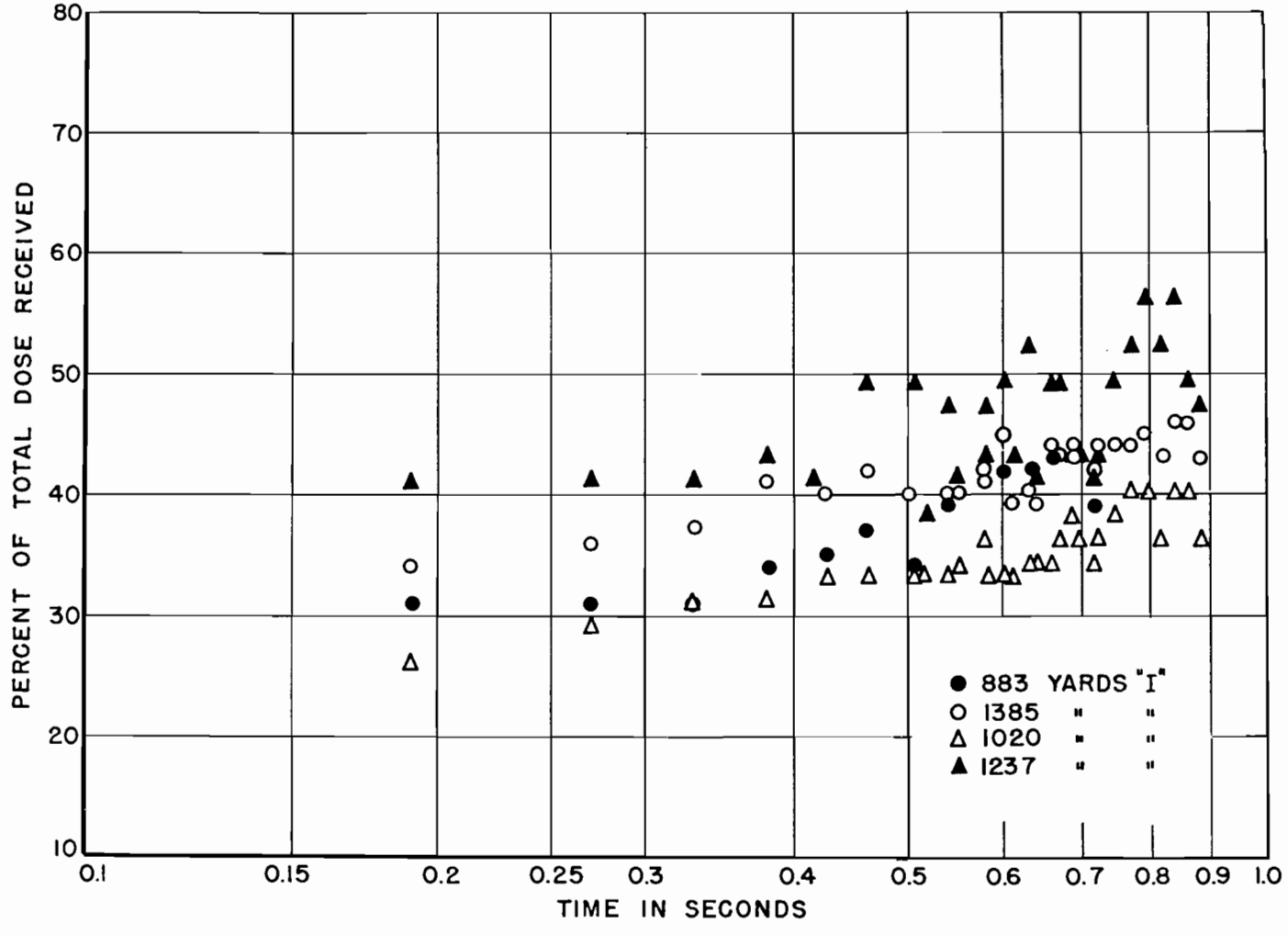

Fig. 6.6 Percentage of Film Dose Received at Various Times—Flash Initiated Film Drops

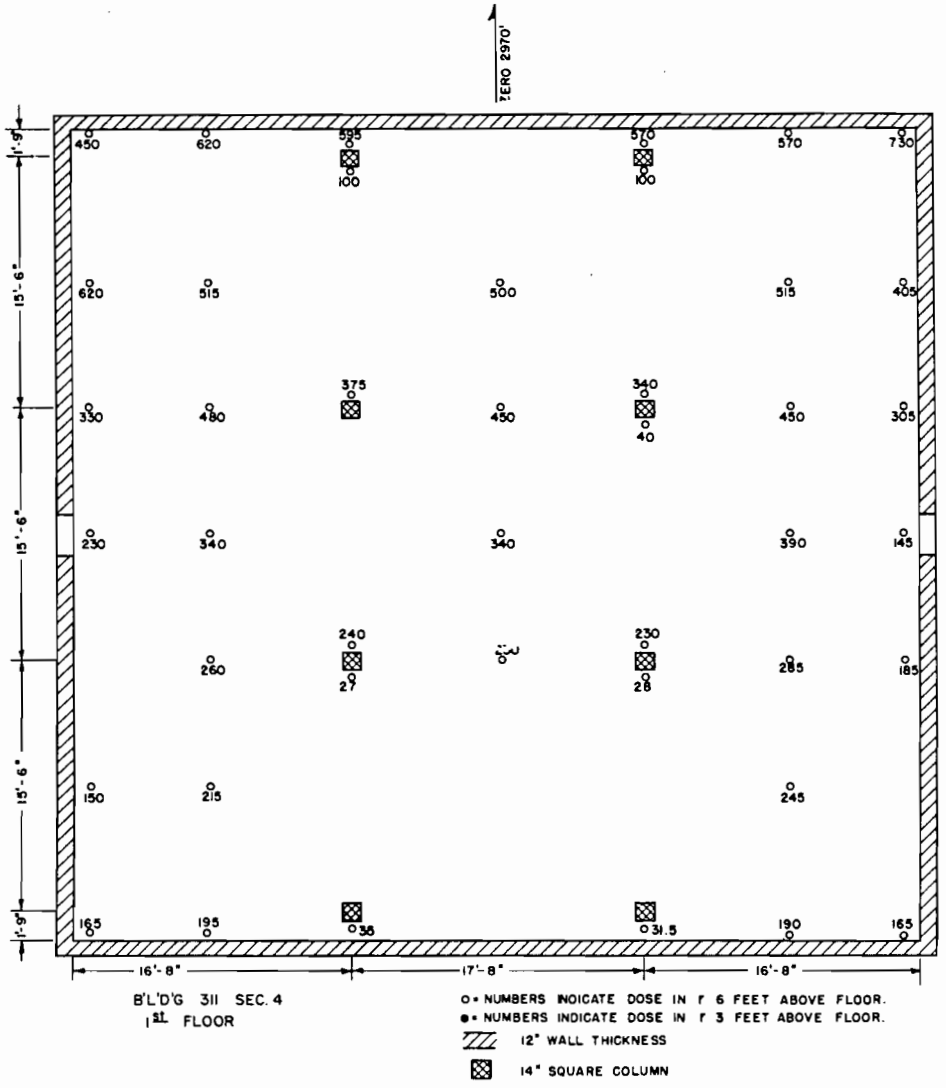

Fig. 6.7 Schematic of First Level, Building 311

[redacted]

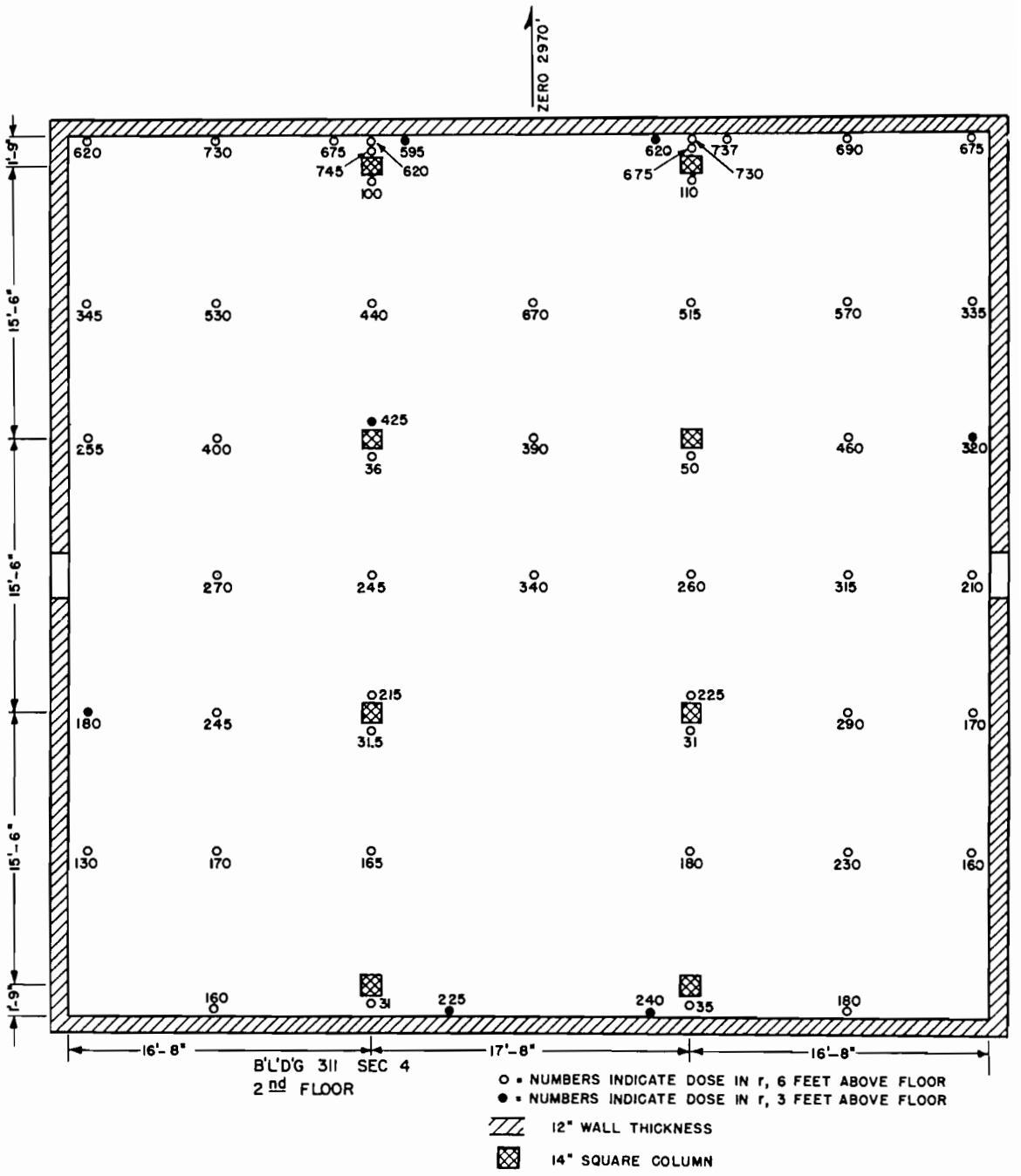

Fig. 6.8 Schematic of Second Level, Building 311

[redacted]

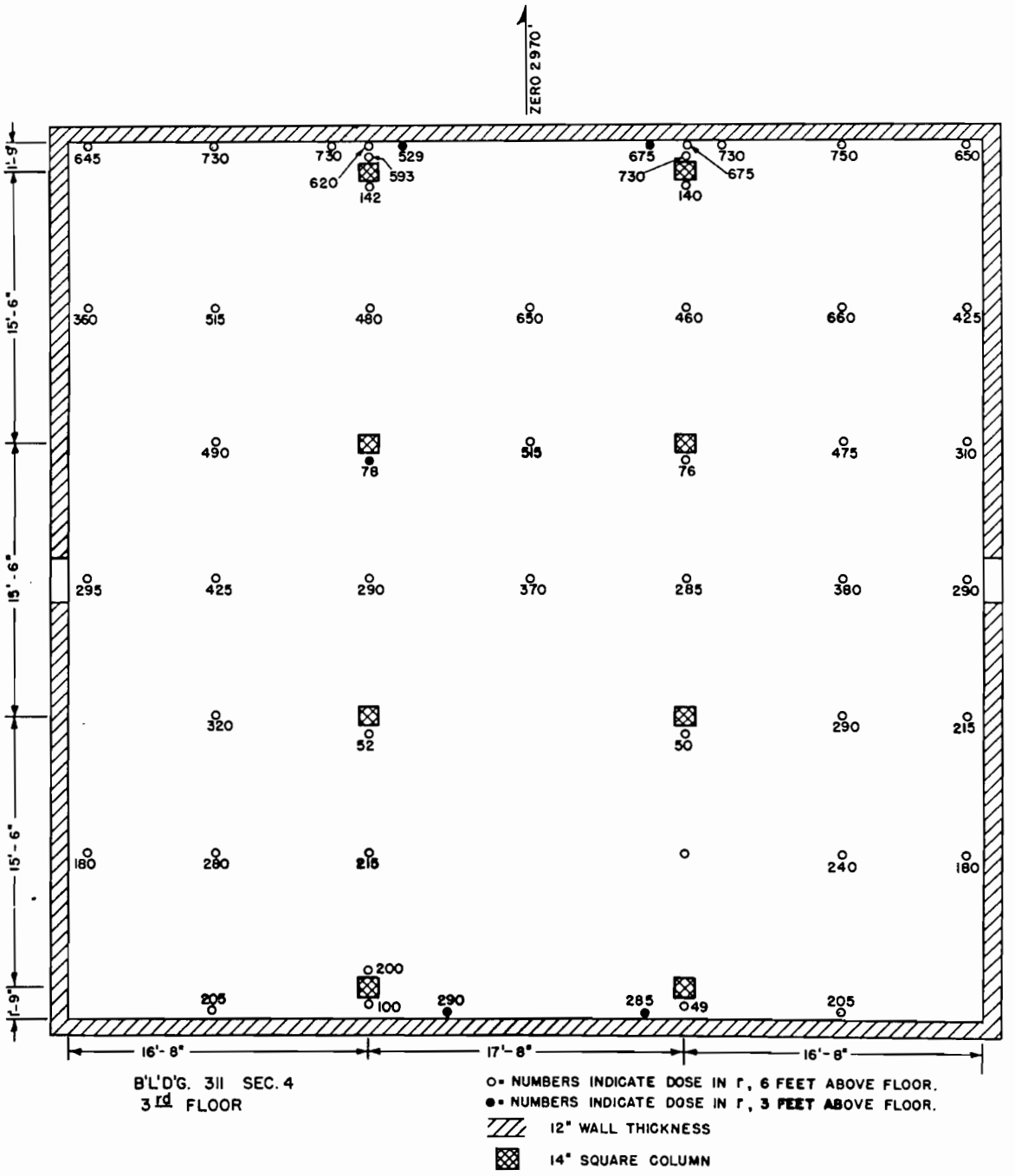

Fig. 6.9 Schematic of Third Level, Building 311

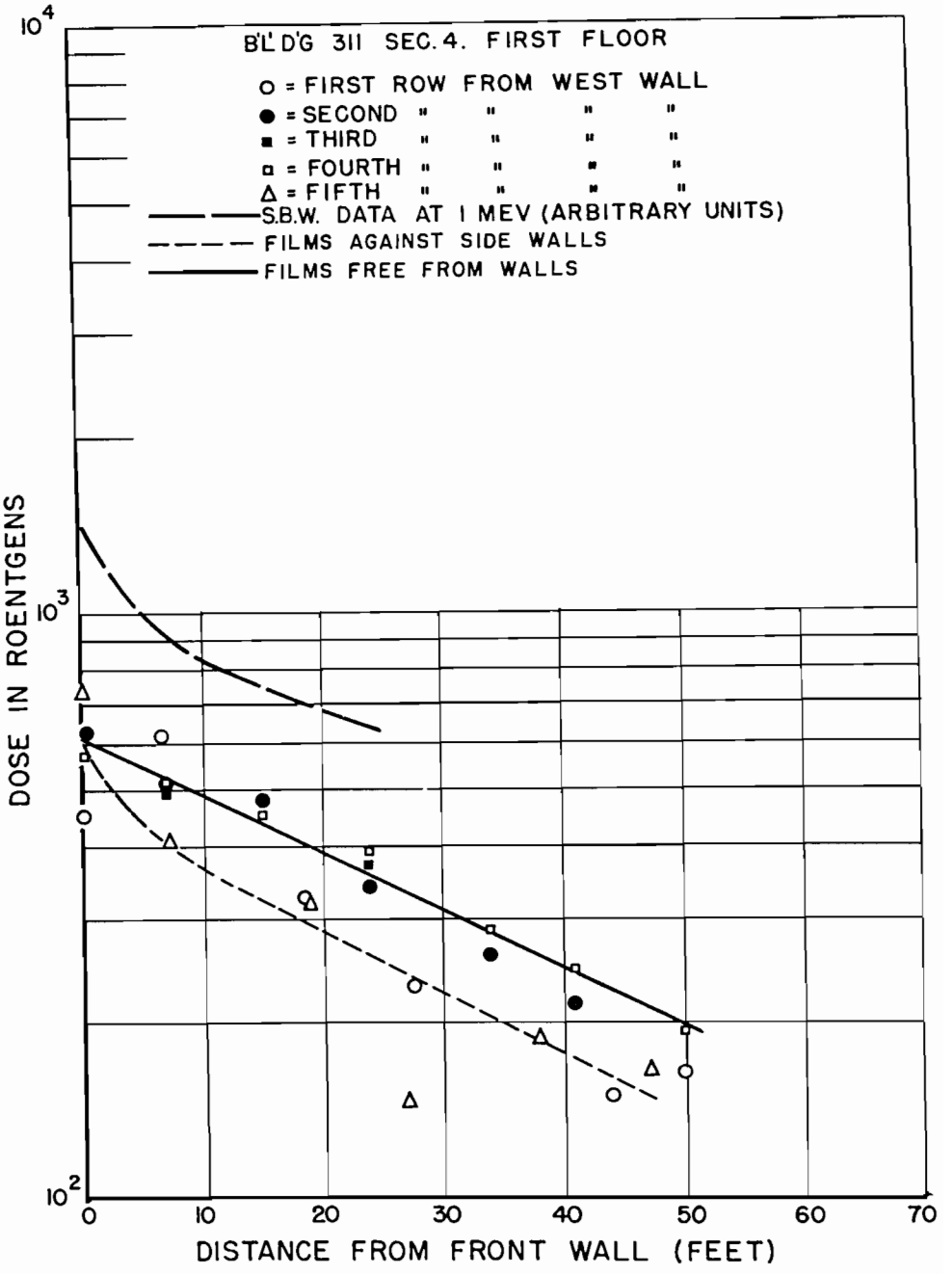

Fig. 6.10 Dose in Building 311, First Floor

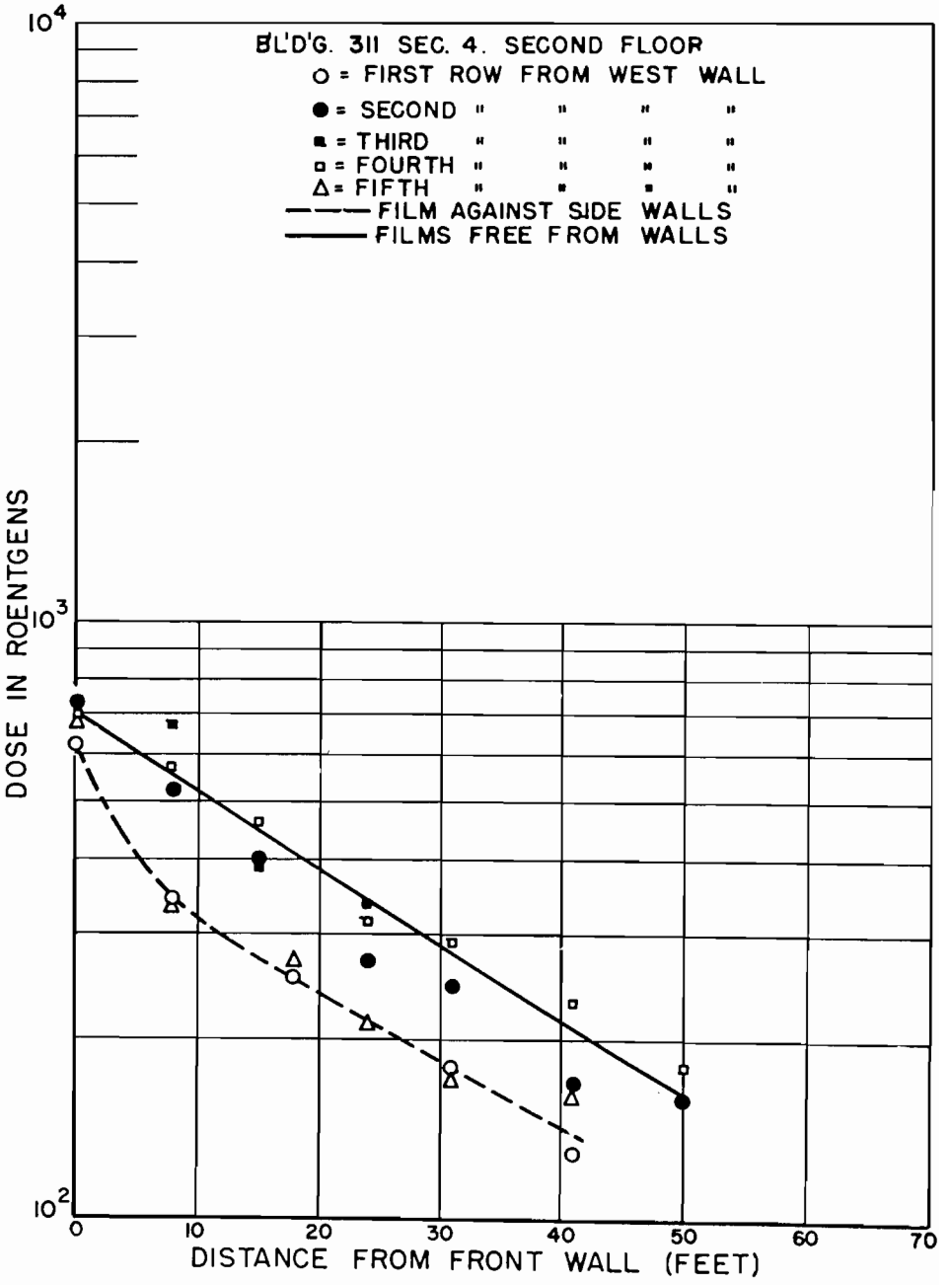

Fig. 6.11 Dose in Building 311, Second Floor

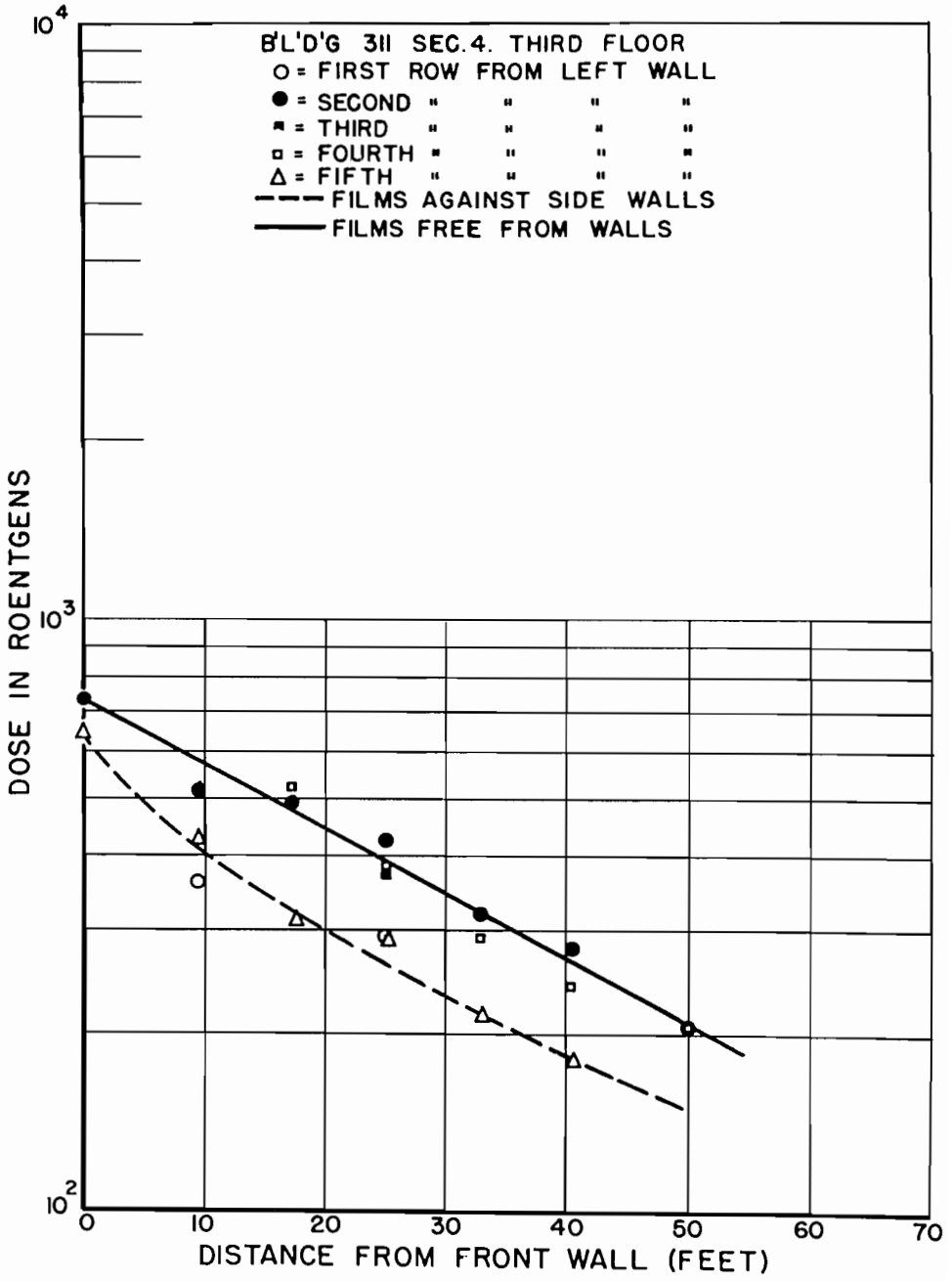

Fig. 6.12 Dose in Building 311, Third Floor

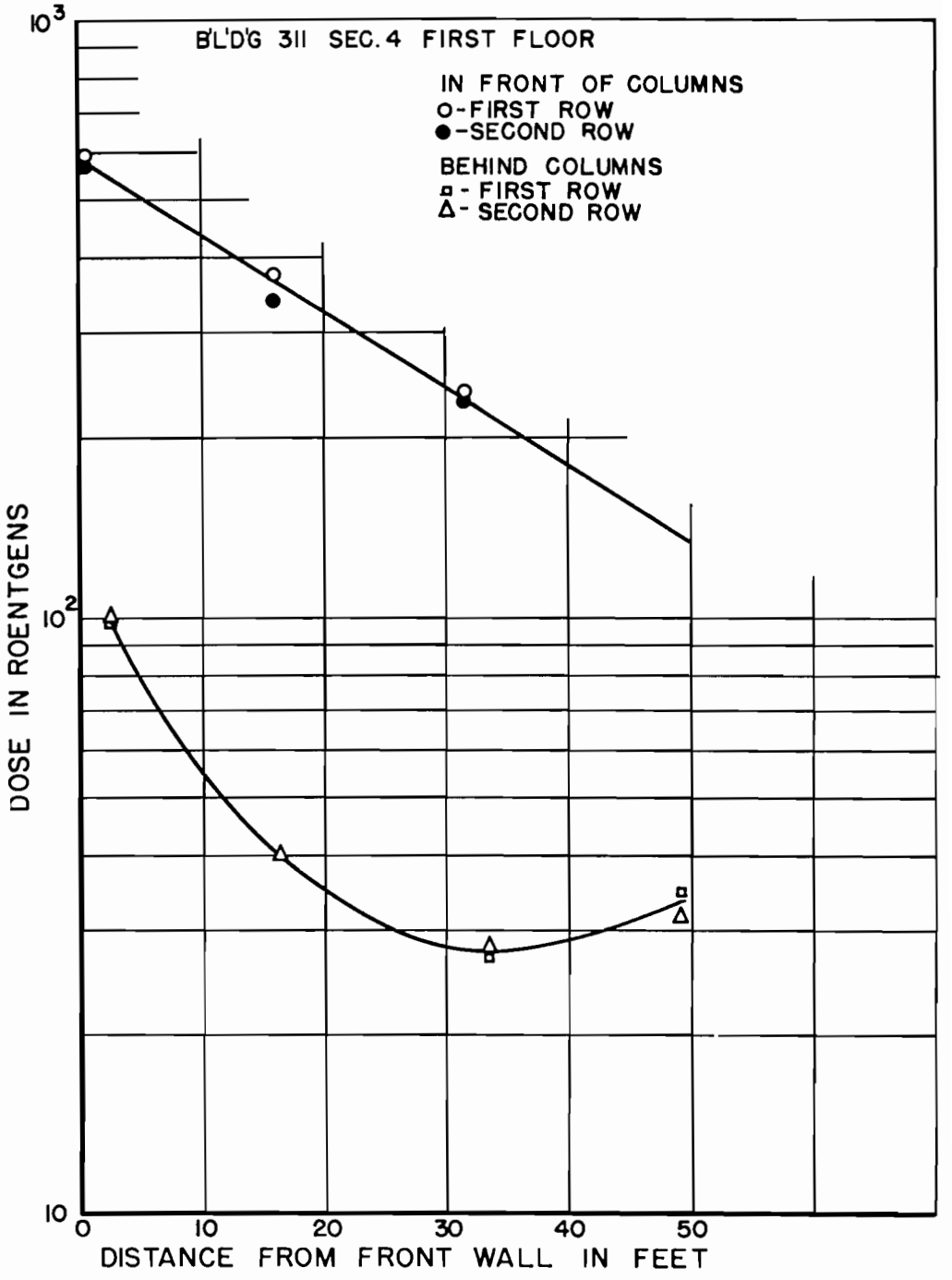

Fig. 6.13 Dose in Building 311, First Floor; Dosimeters Placed at Front and Rear of Columns

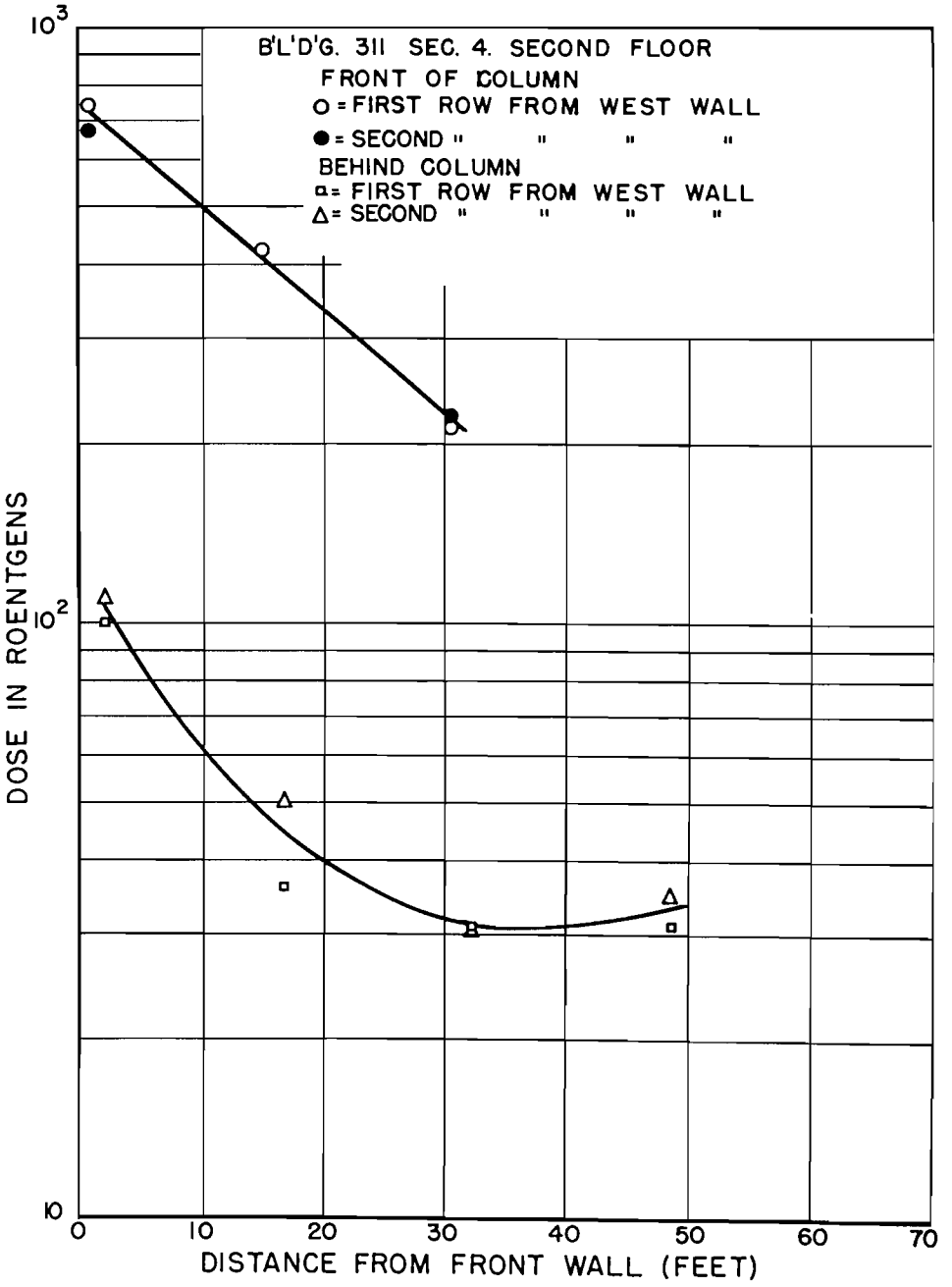

Fig. 6.14 Dose in Building 311, Second Floor; Dosimeters Placed at Front and Rear of Columns

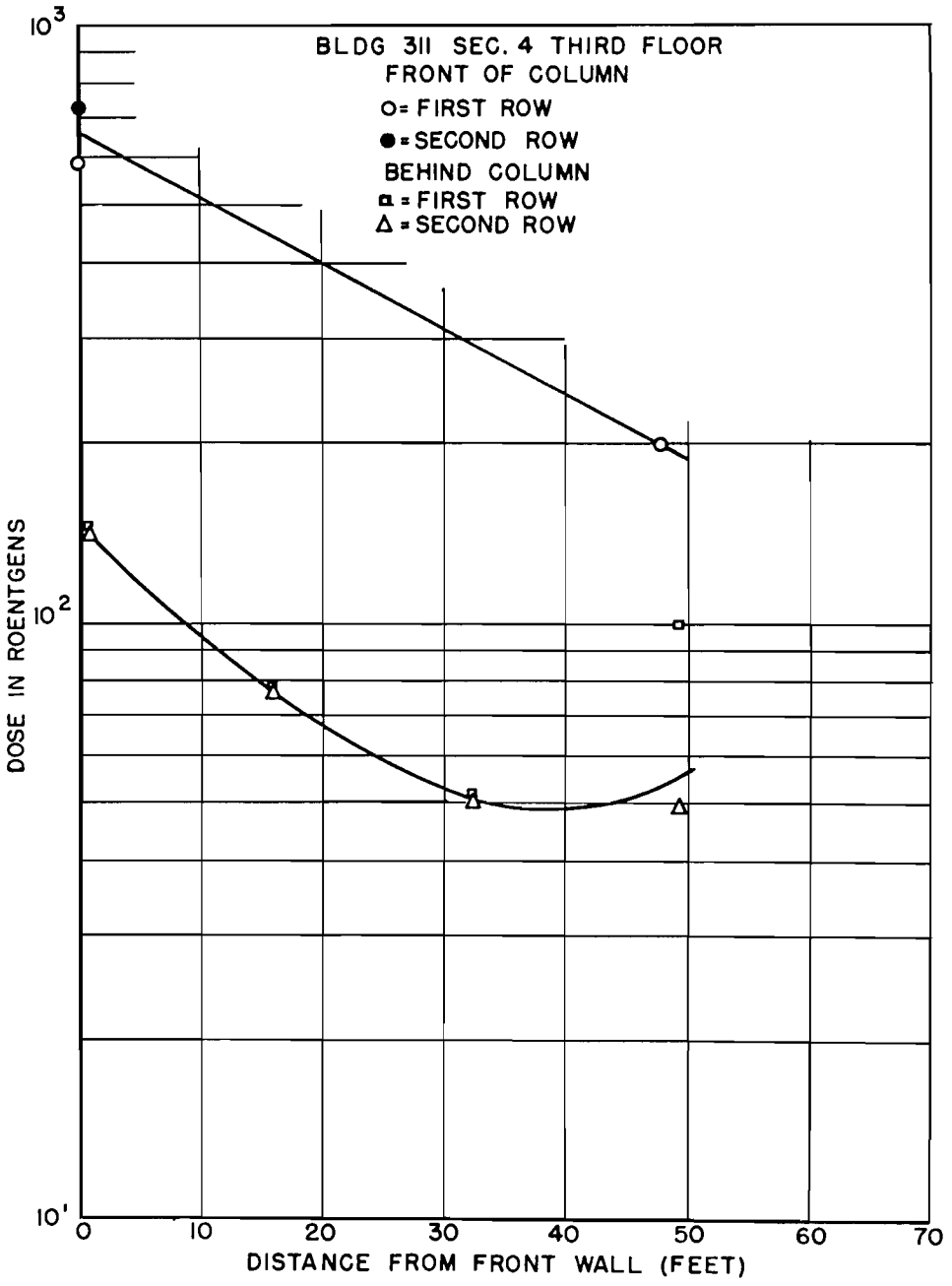

Fig. 6.15 Dose in Building 311, Third Floor; Dosimeters Placed at Front and Rear of Columns

approach to narrow-beam attenuation in the front wall.[2]

Figures 6.13, 6.14, and 6.15 give similar results for those films which were placed immediately in front of or back of the 1 ft square columns.

REFERENCES

1. L. V. Spencer and U. Fano, Phys. Rev., 81: 464-466 (1951).
2. G. Singer, C. B. Braestrup, and H. O. Wyckoff, Am. J. Roentgenol. Radium Therapy, 56(6): 771 (1946).

AEC, Oak Ridge, Tenn., A31974